Master's Thesis

Enhancing Post-Harvest Preservation through Improved and Even Solar Drying: A Case Study in Bhutan

by Lara Constanze Müller

LUND UNIVERSITY

LTH
FACULTY OF
ENGINEERING

Lara Constanze Müller

Enhancing Post-Harvest Preservation through Improved and Even Solar Drying: A Case Study in Bhutan

Thesis for the degree of Master of Science in Sustainable Energy Engineering

Department of Energy Sciences
Faculty of Engineering, LTH
Lund University

Supervisor: Dr. Henrik Davidsson
Co-Supervisor: Samten Lhendup
Examiner: Prof. Martin Andersson

June 2024

Acknowledgement

Abstract

This thesis investigates the enhancement of solar drying techniques for agricultural produce, focusing on achieving uniform drying to reduce post-harvest losses. Conducted in Bhutan, a developing country in the Himalayas with abundant sunlight but limited preservation infrastructure, the study aimed at constructing an efficient and affordable solar dryer. The primary objectives were optimizing airflow, assessing component performance, and ensuring cost-effectiveness using locally available materials.

The research combines theoretical analysis with extensive experimental data collected in Dewathang, Bhutan. The results indicate that fan configuration is crucial for the efficiency and uniformity of drying in solar dryers. Utilizing reversible fans showed promising outcomes due to their ability to adjust airflow direction, enhancing drying rates.

Comparing the drying processes of bananas and chilies demonstrated that different produce require specific settings to achieve optimal results. In general, the experiments revealed a tradeoff between short drying times and uniformity and a strong dependence on external parameters such as solar irradiance.

Overall, the findings suggest that while the current solar dryer design is promising, further improvements are necessary to achieve uniform drying across various climatic conditions. This thesis provides key insights into airflow optimization, component efficiency, and practical recommendations for future development, contributing to the sustainable preservation of agricultural produce in Bhutan and similar regions.

Table of Contents

I   List of Figures

II   List of Tables

1 Introduction and Objective

The development of efficient food preservation methods remains challenging, particularly in regions like Bhutan where agricultural practices are widespread but preservation infrastructure is lacking. Solar food dryers harness the abundant sunlight providing a means to preserve surplus agricultural produce, and increase its shelf life while maintaining nutritional values. (Joardder and Hasan Masud, 2019)

This master's thesis addresses the enhancement of solar food drying techniques, with a specific focus on achieving uniform drying to reduce post-harvest losses. Drawing from prior research in this domain, it's evident that solar drying presents a promising solution. However, challenges persist, particularly in achieving uniform drying, which is important for ensuring product quality and market viability. In addition, there are concerns about low drying rates and therefore long drying times that need to be tackled. (Robin, 2023)

Bhutan is a developing country. Hence, affordability and availability of materials are as important to consider as the technical efficiency of the solar dryer. This leads to the objective of finding a compromise between integrating technological advancements and keeping the acquisition and running costs low.

By evaluating the performance of existing solar dryers, this research aims to optimize drying efficiency and uniformity. Through practical experimentation and data analysis, critical questions regarding airflow optimization, component performance, and potential improvements will be addressed.

In the context of agricultural practices in the Himalayan region, where traditional preservation methods such as open-air drying are often inadequate, controlled solar drying emerges as a sustainable alternative. While existing designs have shown promise, there remains a need for refinement to meet the specific requirements of drying fruits and vegetables with varying moisture content. This study entails theoretical considerations yet the main part is the experimental data collection conducted in Dewathang, Bhutan as well as the analysis of the obtained results.

1.1 Project Introduction

This thesis is part of a project called *Solar Food: Reducing post-harvest losses through improved solar drying*. This initiative is dedicated to crafting an affordable solar-driven food dryer with the objective of enhancing food preservation standards in the Himalayan region. It started in 2020 and the initially defined design criteria for the first dryer built were affordability, flexibility, low complexity and sustainability. One of the novelties within this project has been the integration of a heat exchanger in the solar dryer (Probert, 2022).

There have been several iterations and various improvements of the initial design resulting from outcomes of conducted experiments. Further details about the previous designs are presented in Chapter 2.4.2. The focus of this thesis is on the uniformity of the drying process. It will be assessed by applying different ventilation strategies to influence airflow within the dryer.

Several different fruits and vegetables have been dried during past experiments such as apples, ginger and eggplant. During this research, banana and chili have been the chosen produce for drying.

The following research questions serve as guidance throughout the conducted work:

- What adjustments in fan placement and airflow pattern can improve the uniformity of drying rates for different layers of bananas and chilies in a solar dryer operating in Bhutan?
- What are the optimal temperature and humidity conditions for drying bananas and chilies in a solar dryer, and can these conditions be consistently maintained using locally available solar technology?
- How effective is the solar dryer in preserving bananas and chilies compared to traditional open-air drying methods among small-scale farmers in Bhutan?

1.2   Limitations

The following list outlines limitations applying to the study and the conducted experiments:

Geographical and Temporal Limitations
- All experiments for this research were conducted at Jigme Namgyel Engineering College (JNEC) in Dewathang, Samdrup Jongkhar. The town is located in southeastern Bhutan close to the Indian border at an altitude of 880 m (JNEC, 2020) which may limit the generalizability of the findings to other geographical locations with different climatic conditions.
- The experiments were conducted during a specific period (March - April 2024), and the findings do not capture seasonal variability in solar irradiance and ambient temperatures throughout the year.

Methodological and Technical Limitations
- The research was conducted using only two indirect solar dryer designs, which may not fully represent the diversity of solar dryer configurations available.
- Experiments were conducted in a field setting rather than a controlled laboratory environment, limiting the ability to control e.g. environmental variables.
- The study focused exclusively on banana and chili drying. The findings may not apply to other types of agricultural produce that have different drying characteristics.

- The technical equipment available in Bhutan was limited, potentially introducing inaccuracies.
- All weight measurements were conducted manually, which may have introduced human error and inconsistencies in the data.
- The long-term performance and durability of the constructed solar dryers could not be evaluated due to the short duration of the experiments.

Scope and Analysis Limitations

- The study does not include a financial or market analysis.
- External factors such as local socio-economic conditions, policy frameworks, and cultural practices were not investigated but could influence the implementation of solar drying technologies.

Unless otherwise noted, all photographs, figures, and tables in this thesis were taken, created, and edited by the author.

2 Background

2.1 Bhutan

Bhutan is not only located in the Himalayas but it is also the most mountainous country in the world (WorldAtlas, 2024). The South Asian Kingdom of Bhutan borders India in the south and the Tibet province of China in the north. Bhutan's largely agrarian society relies heavily on farming, and agriculture contributes substantially to its economy, providing subsistence to the majority of the population (National Statistics Bureau, 2022). However, the country's rugged terrain, characterized by steep mountain slopes and limited road infrastructure, poses significant challenges to agricultural practices, particularly during the post-harvest phase. Consequently, farms lack market access. Due to irregular rainfalls certain produce can only be planted and harvested at specific times of the year. Bhutan experiences four seasons. The experiments for this thesis were conducted during spring in which temperatures and humidity levels rise and occasional rainfalls occur.

The remote and often inaccessible rural areas, where farming remains the primary source of sustenance, are most vulnerable to post-harvest losses, resulting from inadequate drying and storage facilities. This circumstance is exacerbated due to climate change. Losses impact food security, economic stability, and the overall well-being of the rural population. (Chhogyel and Kumar, 2018)

Currently, around 30 % of Bhutan's comestibles are imported. The Ministry of Agriculture and Forests is aiming to increase national food production in order to reduce the import rate. Therefore, several projects have been started as part of the National Food Security Programme. (Chhogyel and Kumar, 2018)

Bhutan is facing significant challenges related to food insecurity and malnutrition. Nutrient deficiencies, particularly in iron, iodine, and vitamin A affect both children and adults and the situation is even more severe in rural areas where access to food is limited. The National Nutrition Strategy and Action Plan (2021 – 2025) aims at identifying and tackling these challenges. (Ministry of Health Bhutan, 2021)

Bhutan spans across six distinct agroecological zones, characterized by altitudinal variations ranging from 100 m in the south to over 7 000 m in the north (Ministry of Agriculture, 1992). This geographical diversity implies unique climatic conditions and resource availability across different regions.

2.2 Drying as Food Preservation Method

Different types of food require different preservation methods. Storage of common cereal crops in Bhutan, such as rice, maize or wheat is rather straightforward (National Statistics Bureau, 2021). Preservation of produce containing a high amount of water like fruit and vegetables becomes more challenging.

Common preservation techniques in other parts of the world including freezing, aseptic filling or canning are very difficult or even impossible to implement comprehensively in developing countries such as Bhutan (Robin, 2023).

In the Himalayan region, open-air drying is a prevalent method used to enhance the suitability of food for storage. It aims at removing moisture through utilization of solar energy and thereby inhibits water activity (Mat Desa et al., 2019). This involves placing food items, for instance chilies, on open surfaces such as rooftops to be exposed to direct sunlight. While this technique is simple and functional, it comes with several drawbacks. Due to the uncontrollable nature of open-air drying, critical parameters like drying temperature, humidity, and airflow cannot be regulated. Consequently, this process often results in nutrient loss, exacerbating the prevailing issue of malnutrition in Bhutan. Moreover, spoilage rates are high, drying rates are low and there is no protection against rain, dust or insects, further compromising food quality and safety. This method also requires large areas and long drying times to achieve the necessary conditions for storage. (Inyang et al., 2017)

Food dryers offer a promising solution for drying produce in a controlled manner. Among these, electrical hot air dryers stand out for their ability to regulate all relevant parameters of the drying process. However, their high energy consumption poses a significant disadvantage, rendering them comparably unsustainable. (Inyang et al., 2017)

Introducing solar food dryers: Although drying parameters cannot be influenced as precisely as with an electrical hot air dryer, solar dryers avoid the need for external energy supply by harnessing abundant solar energy to dry various produce. In Chapter 2.4 different types of solar dryers are presented and described.

2.2.1 Theoretical Background on Drying Characteristics

During the experiments bananas and chilies were dried. According to literature, ideal drying temperatures in general and for these food items are between 50 °C – 60 °C and a suitable relative humidity (RH) level lies around 30 % – 40 % (Dandamrongrak et al., 2003; Getahun et al., 2021). Temperatures as well as RH values were measured during the experiments. RH is a measure of the amount of moisture in the air relative to the maximum amount of moisture the air can hold at a certain temperature, expressed as a percentage. It indicates how close the air is to being

saturated with moisture. Relative humidity is affected by both the absolute humidity (AH) content in the air and the air temperature. Warmer air can hold more moisture than cooler air at the same relative humidity. In order to compare humidity levels at different temperatures, it is relevant to determine AH in $^g/_{m^3}$. This can be done by using psychrometric charts or the following equations (Wagner and Pruss, 1993):

$$AH = \frac{RH \cdot p_s}{R_w \cdot T \cdot 100}$$
(2.1)

where:

p_s = saturation vapor pressure in Pa; $R_w = 461.5 \frac{J}{kg \cdot K}$= specific gas constant for water vapor; T = temperature

$$p_s = p_c \cdot exp\left[\frac{T_c}{T}\left(\begin{matrix}a_1\tau + a_2\tau^{1.5} + a_3\tau^3 + \\ a_4\tau^{3.5} + a_5\tau^4 + a_6\tau^{7.5}\end{matrix}\right)\right]$$
(2.2)

where:

$p_c = 22.064$ MPa = critical pressure for water; $T_c = 647.096$ K = critical temperature for water; $\tau = \frac{T}{T_c}$; $a_1, a_2, a_3, ..$= empirical constants (Wagner and Pruss, 1993)

Although optimal drying temperature and humidity are similar for both produce, other characteristics differentiate between banana and chili. Specifically, drying rate and time required for the food to reach a safe moisture content for storage vary significantly. Literature suggests that bananas are safe to store with a moisture content of about 25 % (dry basis) which can be reached after approximately 20 hours of drying (Dandamrongrak et al., 2003). Chilies, on the other hand, need to be dried to moisture contents around 12 % (dry basis) to be safe for storage. This can take around 70 hours of drying (Getahun et al., 2021).

These parameters do not only vary with type of food. They also vary for different maturity stages of the same kind of food. However, no reliable information on drying parameter changes for different maturity levels could be found in the literature.

There are different ways of calculating and expressing drying rates. The following equation 2.3 has been used in this thesis. It expresses the lost weight due to moisture evaporation per hour and surface area in $^g/_{h \cdot m^2}$.

$$drying\ rate = \frac{\Delta m}{\Delta t \cdot A}$$
(2.3)

2.3 Heat and Mass Transfer

During food drying, heat and mass transfer mechanisms take place. Heat transfer happens mainly from the heat source to the food inside the dryer. Mass transfer, dominantly in form of diffusion, occurs inside and outside the drying food product. (Getahun et al., 2021; Srikiatden and Roberts, 2007)

Performance of a solar dryer depends not only on its capacity to harness solar energy but also on the extend of associated losses. Therefore, it is important to understand the involved processes for optimizing drying efficiency and preserving food quality.
The three different modes of heat transfer within solar dryers are conduction, convection and radiation.
Conduction refers to transferring heat through solid materials. This takes place through the wooden structure of the solar dryer. As thicker walls lead to reduced losses, it is beneficial to not only consider material thickness itself but also adding insulation layers to the design.

Convective heat transfer takes place in fluids such as air in this case. It is relevant for every component of a solar dryer as air travels through each of them. Especially the efficiency of the incorporated heat exchanger depends on the convective heat transfer rate and minimizing losses. Convection can be separated into natural and forced convection. The difference is that while natural convection is driven only by density differences, forced convection involves external forces to increase heat transfer. (Çengel and Ghajar, 2020)

Radiative heat transfer occurs through electromagnetic waves. In this context, solar radiation is harnessed to increase the temperature inside the dryer and eventually dry the food items.

Mass transfer processes, such as diffusion and evaporation, are relevant when looking at moisture removal from food during drying. Diffusion lets moisture move from regions of higher concentration to lower concentration within the food, while evaporation is responsible for the conversion of liquid water into vapor. The rate of mass transfer is influenced by factors such as temperature, humidity, and airflow within the drying chamber. (Srikiatden and Roberts, 2007)

2.3.1 Heat Transfer Rate

While Q indicates the sheer amount of transferred heat in Joule, the heat transfer rate $\dot{Q}$ expresses the amount of heat transferred per unit time in $J/_s = \text{Watt}$ (Çengel and Ghajar, 2020). During the experiments, solar irradiance is measured in $W/_{m^2}$, also called solar flux.

The respective heat transfer rate can be estimated by simply multiplying this value by the absorber area.

The solar dryer system is considered a stationary closed system involving only heat transfer. The following equation 2.4 expresses the conservation of energy relation.

$$\dot{Q} = \dot{m} \cdot c_p \cdot \Delta T \tag{2.4}$$

where:

$\dot{m}$ = mass flow rate in $\frac{\text{kg}}{\text{s}}$; $c_p = 1.006 \frac{\text{kJ}}{\text{kg·K}}$ = specific heat capacity of air; ΔT = temperature difference before and after control volume (closed system)

$$\dot{m} = \rho \cdot V \cdot A_c \tag{2.5}$$

where:

ρ = air density; V = inlet airflow velocity; A_c= cross-sectional area of inlet

In order to calculate air density, air pressure at the altitude the experiments took place needs to be estimated using the barometric formula expressed in equation 2.6 (Atkins et al., 2018).

$$p = p_0 \cdot \exp\left[\frac{-g \cdot M \cdot (h - h_0)}{R \cdot T}\right] \tag{2.6}$$

where:

$p_0 = 1\,\text{atm}$ = air pressure at sea level; $g = 9.81 \frac{\text{m}}{\text{s}^2}$ = force of gravity; $M = 0.029 \frac{\text{kg}}{\text{mol}}$ = molar mass of air; h = altitude; $h_0 = 0\,\text{m}$ = reference altitude; $R = 8.31 \frac{\text{Nm}}{\text{mol·K}}$ = universal gas constant; T = temperature at altitude h

Dewathang is located at an altitude of approximately 880 m (JNEC, 2020) which gives an air pressure of $p = 0.9\,\text{atm}$ and consequently an air density of $\rho = 1.05 \frac{\text{kg}}{\text{m}^3}$.

2.4   Solar Dryers

2.4.1 Solar Dryer Classification

In general, solar dryers can be classified based on two main factors: the mode of air circulation and the solar contribution to the system. Air circulation can be passive (natural convection) or active (forced convection) as explained in the previous chapter. The difference is that active circulation incorporates fans to enhance the airflow inside the dryer rather than relying on natural air density differences.

Within both active and passive dryer types, various heating methods can be employed. In direct

solar dryers, produce is positioned beneath transparent covers, allowing solar radiation to directly heat the surface of the food. On the other hand, there are indirect solar dryers where comestibles are placed in drying chambers and heated air is used for drying instead of direct radiation. This type of dryer is particularly suitable for perishable fruits susceptible to changes in nutritional content and color due to exposure to sunlight (Ekechukwu and Norton, 1999). Latter are considered more efficient as higher drying rates and a more uniform drying can be achieved. In addition, nutritional value of the dried food is higher since the produce is not exposed to direct solar radiation (Kumar et al., 2016).

2.4.2 Solar Dryers within the Project

All dryers within the project have been indirect solar food dryers. The initially designed dryer within the project was the first of its kind to incorporate a heat exchanger. In addition, the solar absorber was placed on top of the drying chamber achieving a compact design and further increasing efficiency (Probert, 2022).

The design evolved and features such as an internal fan were added by building upon results from field tests (Probert, 2022). The most recent version of this dryer can be seen in Figure 2-1 and Figure 2-2.
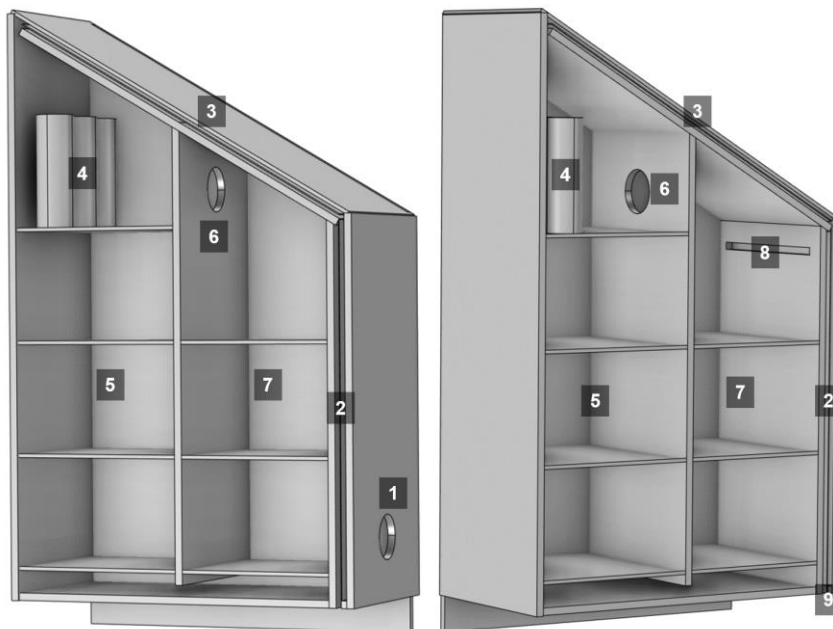
Figure 2-1: CAD model of dryer's initial design [adapted from (Rissler, 2023)]

Figure 2-2: Photo of dryer's initial design in Bhutan

Components shown in Figure 2-1, Figure 2-2, Figure 2-3 and Figure 2-4: 1 – Inlet, 2 – Heat exchanger, 3 – Absorber, 4 – Heat storage, 5 – Drying chamber 1, 6 – Partition with internal fan, 7 – Drying chamber 2, 8 – Drying chamber outlet, 9 – Outlet

One year later, based on suggestions from conducted experiments, the dryer's design was updated and a first version was built in Lund (Jamtsho and Om, 2023). Table 2-1 presents an overview of the central characteristics of each dryer. The main changes are an enlarged absorber and relocation of the heat exchanger. The following Figure 2-3 and Figure 2-4 show the improved model of the dryer. The numbering corresponds to that in the previous illustrations.

Figure 2-3: CAD model of dryer's improved design in Lund [adapted from (Jamtsho and Om, 2023)]
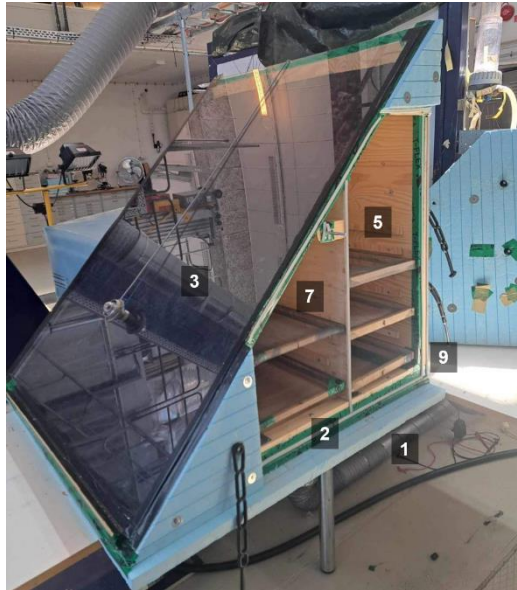
Figure 2-4: Photo of dryer's improved design in Lund

Table 2-1: Comparison of initial and improved solar dryer design

	Initial design	Improved design (in Lund)
Outer dimensions	$1.67 \text{ m} \cdot 0.95 \text{ m} \cdot 0.54 \text{ m}$	$1 \text{ m} \cdot 1 \text{ m} \cdot 1 \text{ m}$
Inlet location	Frontside	Bottom side
Outlet location	Frontside	Backside
Heat exchanger location	Frontside	Bottom side
Heat exchanger area	0.45 m^2	1 m^2
Heat exchanger material	Metal	Polyethene
Absorber area	0.5 m^2	1.4 m^2

2.4.3 Components

Although the designs have changed, the dryer's components remained the same. The following chapter explains the most relevant ones and how they have changed.

15

Heat exchanger

The heat exchanger is the first and last component of the solar dryer. Cold inlet air enters at one side of the counter-flow heat exchanger and after passing through all other components hot air enters at the other side. As the air flows in opposite directions, heat is transferred from hot to cold air through the core of the heat exchanger increasing the dryer's efficiency. This heat transfer occurs due to the temperature difference between the two airflows.

The so-called heat transfer effectiveness ε is defined as follows (Çengel and Ghajar, 2020):

$$\varepsilon = \frac{\dot{Q}}{\dot{Q}_{max}} = \frac{Actual\ heat\ transfer\ rate}{Maximum\ possible\ heat\ transfer\ rate} \tag{2.7}$$

with:

$$\dot{Q} = \dot{m} \cdot c_p \cdot \left(T_{cold,out} - T_{cold,in}\right) = \dot{m} \cdot c_p \cdot \left(T_{hot,in} - T_{hot,out}\right) \tag{2.8}$$

and:

$$\dot{Q}_{max} = \dot{m} \cdot c_p \cdot \left(T_{h,in} - T_{c,in}\right) \tag{2.9}$$

leading to:

$$\varepsilon_{cold} = \frac{\left(T_{c,out} - T_{c,in}\right)}{\left(T_{h,in} - T_{c,in}\right)} \tag{2.10}$$

$$\varepsilon_{hot} = \frac{\left(T_{h,in} - T_{h,out}\right)}{\left(T_{h,in} - T_{c,in}\right)} \tag{2.11}$$

Equation 2.7 is considering an ideal case neglecting potential leakages by assuming that $\dot{m}_{cold} = \dot{m}_{hot}$. Due to practical limitations, it is not possible to measure the mass flow on the hot side of the heat exchanger. Transposing equation 2.8 as follows, makes it possible to estimate flow and leakages as all other values can be measured.

$$\frac{\dot{m}_{hot}}{\dot{m}_{cold}} = \frac{\Delta T_{cold}}{\Delta T_{hot}} \tag{2.12}$$

Absorber

After leaving the cold side of the heat exchanger, air enters the solar absorber and travels towards the drying chamber. The solar dryer's absorber is a metal sheet painted black on both sides and covered by glass, positioned on top of the drying chamber. There are two flow paths, one between the metal absorber core and glass plate and one below the absorber core. Solar radiation is harnessed through radiative heat transfer in the absorber. Painting both sides black ensures that

thermal energy is emitted in both directions. This design allows heat to be emitted towards the drying chamber, enhancing the drying process by contributing additional heat to the food inside.

Initially, the absorber area measured 0.5 m^2. Experiments revealed that increasing the area would significantly improve the drying rate (Rissler, 2023). A first attempt to improve the absorber's performance was to add a metal net for artificial roughness. In practice, improvements caused by this change could not be proven (Mahmoodi, 2023). Therefore, the new dryer design features a larger absorber with an area of 1.4 m^2. The distance between absorber and glass plate, as well as absorber and base remained at 1 cm.

The absorber's efficiency is calculated based on equations 2.4 and 2.7 as follows:

$$\eta_{Absorber} = \frac{Actual\ heat\ transfer\ rate}{Maximum\ possible\ heat\ transfer\ rate} = \frac{\dot{m} \cdot c_p \cdot (T_{Abs,out} - T_{Abs,in})}{G \cdot A_{Absorber}} \qquad (2.13)$$

where:

G = solar irradiance in $\frac{\text{W}}{\text{m}^2}$

Heat storage

While entering the drying chamber, air passes the heat storage comprising of plastic bottles filled with water. The purpose of this optional and removable component is to regulate temperatures throughout the day, preventing the dryer from overheating and thereby safeguarding the food from degradation. Additionally, it facilitates the warming of air later in the day when solar heat may be insufficient, ensuring a consistent and dependable drying process (Rissler, 2023).

Drying chamber

Inside the drying chamber, the harnessed solar radiation is utilized to evaporate the food's moisture. Initially, the drying chamber was one open space housing trays with the produce to be dried. Uneven drying turned out to be an issue. Consequently, the chamber was divided into two separate spaces with a partition, including an internal fan, in between. This way, the airflow inside the dryer could be increased.

External and internal fans

The first design only used an external fan for air intake (Probert, 2022). In order to increase airflow and therefore improve the drying rate, an internal fan was added. It enables internal circulation. Over time, it became evident that a bigger internal fan leads to an increase in drying performance (Jamtsho and Om, 2023; Rissler, 2023).

The internal fan has a significant influence on the evenness of the drying process which is a focus of this thesis. Previously, there have been issues with discrepancies in drying rate between trays

(Jamtsho and Om, 2023; Probert, 2022; Rissler, 2023). Therefore, several different internal fan setups were compared during the conducted experiments as explained in Chapter 3.2.1.

2.5 Uniform Drying

In addition to previously discussed drying performance metrics such as drying rate and drying time, the conducted experiments had a special focus on achieving uniform and even drying across the different food trays inside the solar dryer. The main issue is that while inlet air has a low humidity content and a high temperature, it picks up moisture while traveling through the dryer and ends up in high humidity levels and lower temperatures (Davidsson et al., 2017). Therefore, trays located at the top and therefore closest to the inlet, have best possible drying conditions.

In previous data collections, the primary objective was to optimize the drying process as such and maximize the efficiency of the dryer. However, it becomes evident that achieving rapid drying in some trays, resulting in quick attainment of the required moisture level for safe storage is insufficient if other trays still retain significant moisture content. This appears to be consistent with findings in other studies related to solar drying, as literature addressing the specific issue of uniform drying has been notably scarce.

One potential solution involves rotating the position of trays during the drying process (Davidsson et al., 2017). However, this approach is labor- and time-intensive and can result in losses due to the need to open the dryer.

Alternatively, adjusting the airflow within the dryer presents another possibility. The aim of this approach is to redistribute the airflow so that the low-moisture, high-temperature inlet air can reach all trays more effectively. To investigate this method, various fan configurations were installed and tested during the experiments, as discussed in more detail in Chapter 3.2.1.

Nonetheless, it is important to maintain the objective of designing a solar dryer that is both efficient and cost-effective, keeping complexity low.

3   Method

3.1   Preparations and Verification

Before departing to Bhutan, an extensive literature review has been conducted in order to obtain a comprehensive picture of what has been done within the project, and field in general.

In addition, first tests on the equipment and the previously described solar dryer located in the solar lab at LTH in Lund were made. Thermocouples, which are pairs of different wire materials joined at one end to measure temperatures through electromotive force, were connected to a Campbell Scientific AM16/32 multiplexer. The multiplexer was then connected to a Campbell Scientific CR1000 data logger which finally sends the data through a Serial RS232 cable to a computer. In addition, four Campbell Scientific HygroVUE Digital Temperature and Relative Humidity Sensors were connected to the data logger and tested.

Upon arrival in Bhutan the previous model of the solar dryer, which had been used for different experiments in the past two years, was inspected. Despite some broken sealings and solder connections the dryer was still very much intact. It was cleaned, and fixed and all thermocouples were connected to the previously mentioned multiplexer and data logger. In addition, a reliable electrical grounding was secured which is crucial for experiments like this, and a Kipp & Zonen CMP3 pyranometer was placed on the absorber to measure solar irradiance during the experiments. With this setup in place some first test experiments could be conducted in order to verify functionality of the sensors, fans as well as data collection equipment. In some locations in the dryer, multiple thermocouples are placed to later calculate an average temperature in these specific places. Making sure these sensors' measurements aligned was also part of the verification process.

In parallel, a new dryer based on the improved design was manufactured. The process is described step by step in the following Chapter 3.2. After its completion, the same functionality verification steps as for the previous model were carried out.

3.2   Design and Manufacturing of Solar Dryer

The design of the new dryer is inspired by, but not identical to the one built in Lund in 2023 described in Chapter 2.4.2. The following Table 3-1 presents differences between these two models.

Table 3-1: Comparison of improved solar dryer design in Lund and Bhutan

	Improved design (in Lund)	**Improved design (in Bhutan)**
Outer dimensions	1 m · 1 m · 1 m	1.3 m · 1 m · 1 m
Plywood thickness	8 mm	20 mm
Heat exchanger material	Polyethene	Metal
Absorber area	1.4 m^2	1.5 m^2
Heat storage	3 · 1.5 l water bottles	10 · 0.5 l water bottles
Internal fan	Fixed	Modular

The following Figure 3-1 and Figure 3-2 show a computer-aided design (CAD) model and photo of the dryer in Bhutan. The numbers represent different components of the dryer described in Table 3-2.
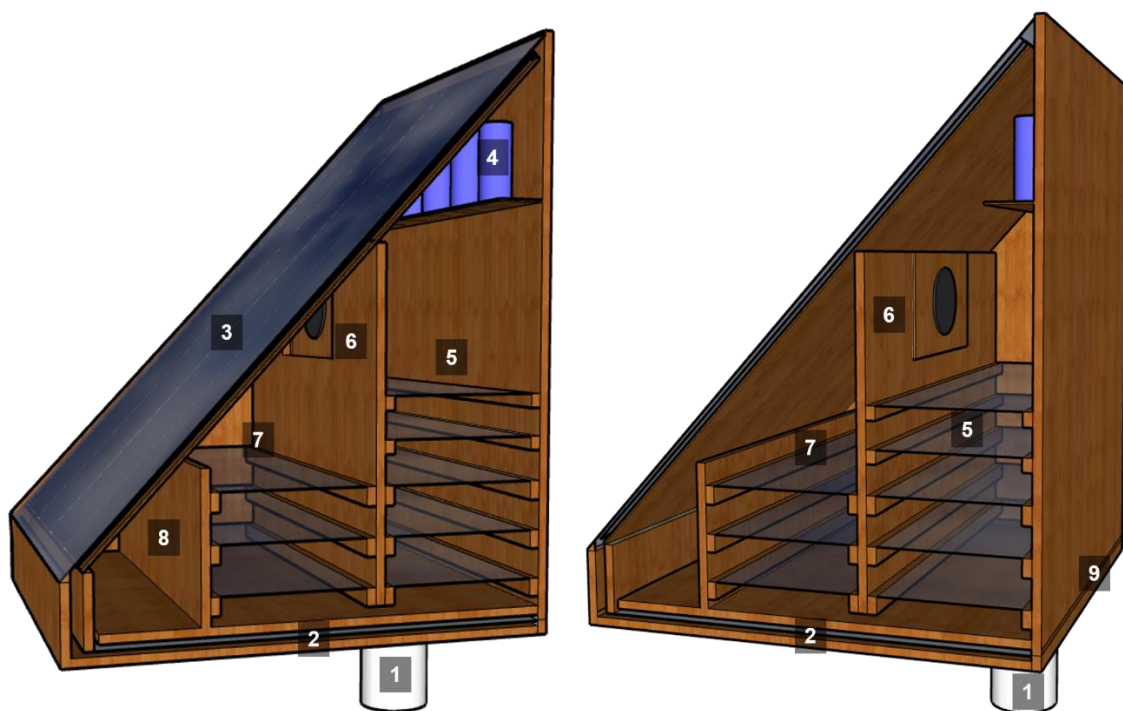
Figure 3-1: CAD model of dryer's improved design in Bhutan [adapted from (Kuepper, 2024)]
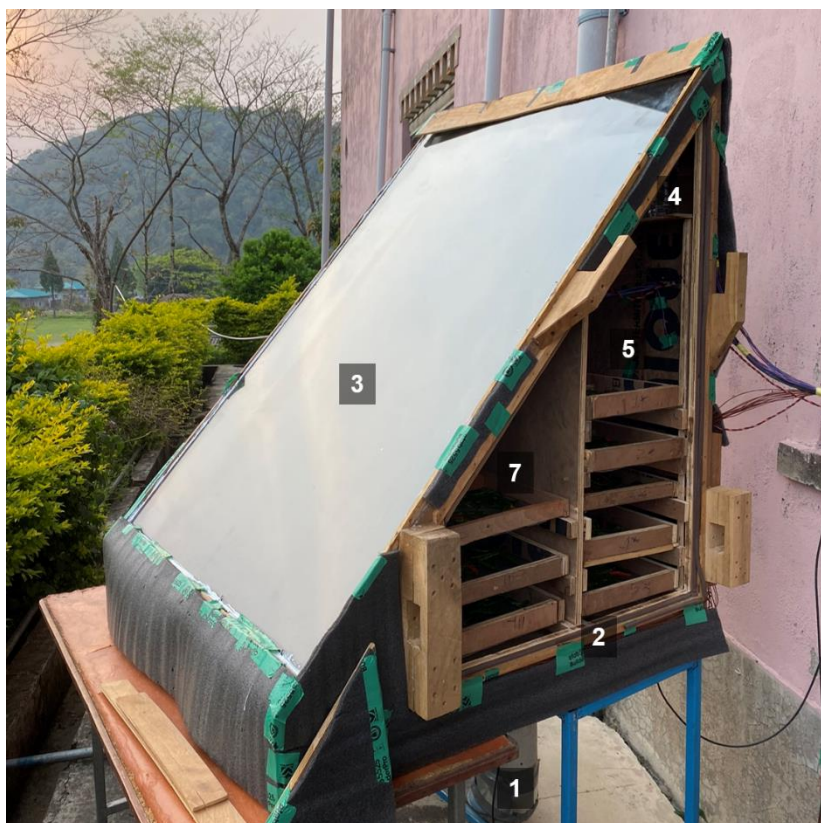
Figure 3-2: Photo of dryer's improved design in Bhutan

The following Table 3-2 provides an overview of the main components, used materials and main measurements.

Table 3-2: Main components, materials and measurements of new solar dryer

No.	Component	Material	Measurements
1	Inlet	Metal and plastic duct	Outer diameter: 160 mm
2	Heat exchanger	Plywood base	Length: 1000 mm Width: 1000 mm Thickness: 20 mm
		Steel core	Length: 800 mm Width: 1000 mm Thickness: 0.25 mm
		Plywood top	Length: 940 mm Width: 1000 mm Thickness: 20 mm
3	Absorber	Plywood base	Length: 1450 mm Width: 1000 mm Thickness: 20 mm
		Steel core	Length: 1450 mm Width: 1000 mm Thickness: 0.25 mm

			Length: 1500 mm Width: 1000 mm Thickness: 5 mm
		Glass top	
4	Heat storage	Plastic water bottles	$10 \cdot 0.5\,\mathrm{l}$
		Plywood shelf	Length: 100 mm Width: 1000 mm Thickness: 5 mm
5	Drying chamber 1	Trays with plywood frame and wire mesh	Length: 300 mm Width: 1000 mm Height: 35 mm
6	Partition 1 with frame for internal fan	Plywood	Length: 750 mm Width: 1000 mm Thickness: 20 mm
7	Drying chamber 2	Trays with plywood frame and wire mesh	Length: 320 mm Width: 1000 mm Thickness: 35 mm
8	Partition 2	Plywood	Length: 320 mm Width: 1000 mm Thickness: 20 mm
9	Back with outlet	Plywood	Length: 1300 mm Width: 1000 mm Thickness: 20 mm

The following manufacturing steps are detailed to ensure reproducibility for future construction of the dryer.

First, plywood panels were sawn into shape. The first component to be built was the heat exchanger as it is the base of the entire dryer. A gap of $10\,\mathrm{mm}$ was kept between the base and metal core. In addition, small wood pieces were placed between the base and core in order to disturb the airflow to thereby increase the heat exchanger's efficiency. On top of that, $10\,\mathrm{mm}$ spacers were placed on the edges to keep a gap on the hot side of the heat exchanger. The top of the heat exchanger serves as the bottom of the drying chambers simultaneously. In order to prevent leakages, it was highly important to seal any unwanted gaps after each manufacturing step. This was either done with a mixture of glue and sawdust, silicone sealant or tape.

In the next step, the back panel as well as the sides (including a door on one side) and the partitions were nailed together. In order to allow airflow from right to left drying chamber, a gap was cut out the bottom edge of the large partition. As it is the goal to use different internal fans during the experiments, a frame was cut out of this partition as well, shown in Figure 3-3. The different fans were screwed onto wooden modules which can then be inserted into the frame during the different setups (see Table 3-3). Further elaboration on the specific fans and setups can be found in Chapter 3.2.1.
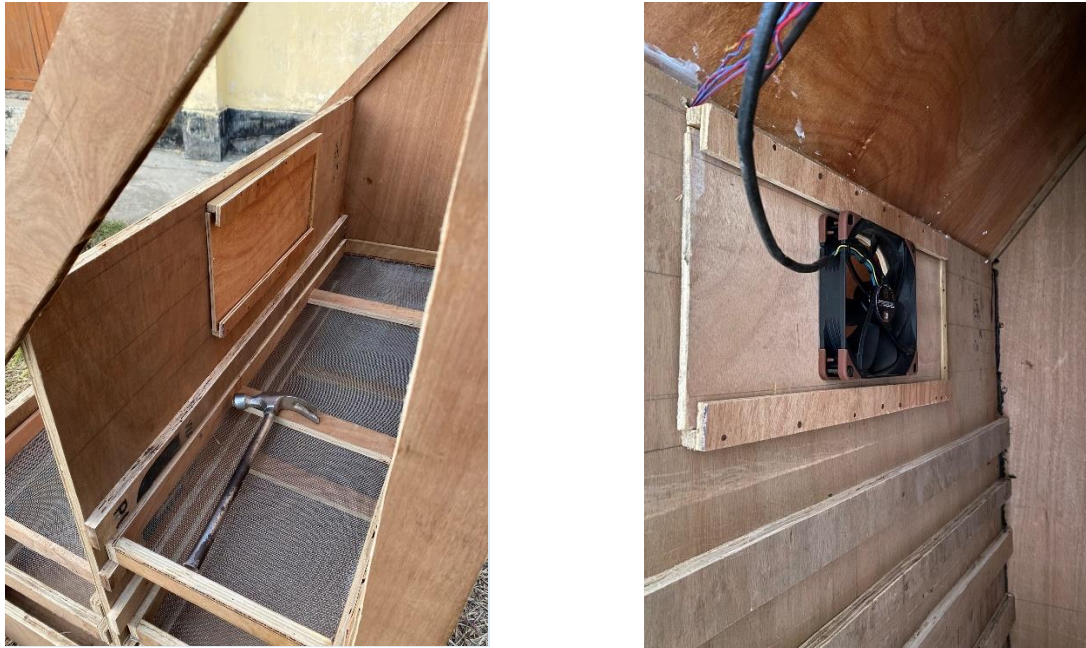
Figure 3-3: Frame for modular fan setups during manufacturing and after completion

Afterward, racks to hold the trays were nailed into the dryer. In parallel, eight trays were assembled and placed inside the dryer. They consist of a wooden frame with stainless steel wire mesh in the center (see Figure 3-4 and Figure 3-5). Moreover, a small rack for the heat storage was placed in the upper part of the right drying chamber. It provides space for ten 500 ml water bottles.

Figure 3-4: Tray arrangement inside dryer

Figure 3-5: Tray made of wooden frame with wire mesh

At this point, the first thermocouples were soldered and placed inside the dryer as they are required in locations that won't be accessible after the next manufacturing steps. Three thermocouples were placed at the inlet of the absorber, three at the outlet of the absorber and three at the inlet of the hot heat exchanger side. When positioning these, it is important to make sure that they do not touch any surfaces or objects. In addition, they should not be placed in direct solar radiation. Therefore, a shading panel (thin plywood plank) was later placed on the top edge of the glass (see Figure 3-2).

Next, the absorber base was positioned on top of the drying chamber. Gaps of $10\,\text{mm}$ for sufficient airflow were kept open. The absorber metal core was painted black from both sides and placed on top of the base with a gap of $10\,\text{mm}$.

After this step, the dryer was moved to its final position for the experiments and the glass top was placed on the absorber. The dryer was positioned so that the absorber faced south. The absorber has an inclination of 46°. As the dryer's inlet is positioned on the bottom, the entire structure was placed on a counter framework. To comply with measurement standards for incoming airflow (Johansson and Svensson, 1999), an extension of the inlet pipe was necessary. Utilizing the same material as the heat exchanger and absorber, a 90° mitered elbow bend was constructed and affixed to the inlet duct. Additionally, the duct was extended beyond the bend using the same material due to unavailability of the $16\,\text{mm}$ duct (see Figure 3-6).

Figure 3-6: Dryer's inlet extension

At this point, the main manufacturing steps were completed and all measurement equipment in and around the dryer was positioned. Figure 3-7 below shows the positions of all 27 thermocouples as well as four relative humidity sensors.
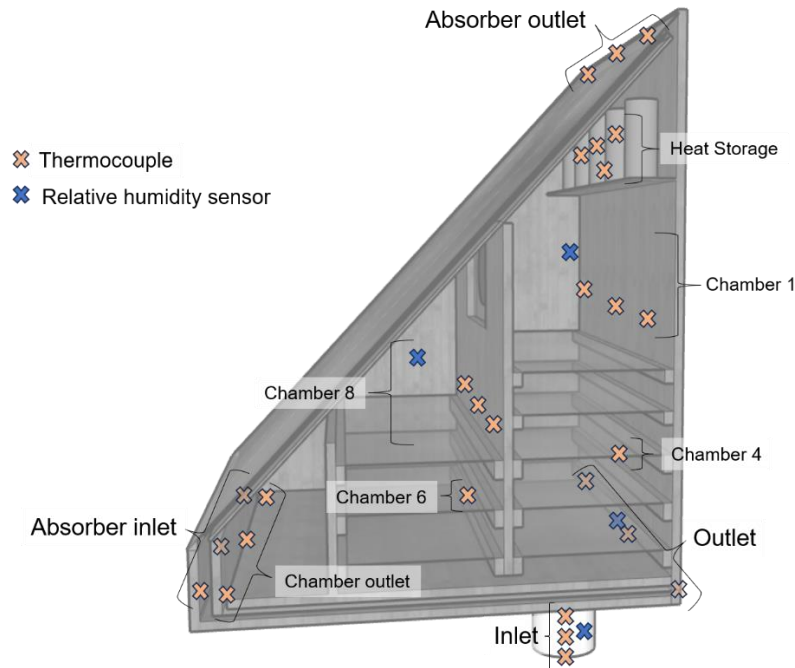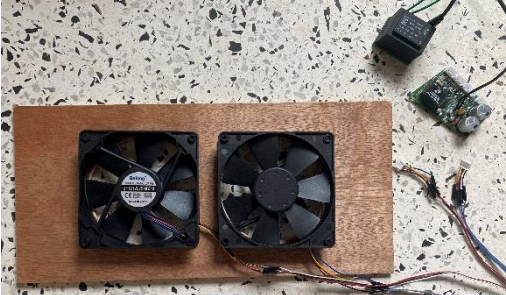
Figure 3-7: Placement of sensors inside and outside of dryer

Next, the external fan was placed right below the dryer's inlet, inside the inlet pipe. As the internal fan is exchangeable, only some permanent electrical connections could be prepared at this point. The final step was the insulation of the dryer to further minimize heat and therefore energy losses as explained in Chapter 2.3. 10 mm thick insulation foam sheets were placed on the bottom, back, both sides and the small area in the front (see Figure 3-2).

3.2.1 Fan Modules and Airflow

Table 3-3 below entails all tested fan setups as well as a short description. Figure 3-8 shows the anticipated airflow pattern for each of the setups. However, these could not be verified as it was not possible to measure the airflow inside the dryer with the available equipment. They are solely based on assumptions. For sketch C, two different flow patterns (yellow and red arrows) were considered possible. Conducting insightful computational fluid dynamics (CFD) analyses on this is subject to further research.

Table 3-3: Fan modules used for internal fan setups

No.	Fan Module	Description
1		Base case scenario without any internal fan **Anticipated airflow pattern: A**
2		NF-A14 industrialPPC-3000 PWM 140 mm · 140 mm · 25 mm Spinning forward **Anticipated airflow pattern: B**
3		NF-A14 industrialPPC-3000 PWM 140 mm · 140 mm · 25 mm Spinning backward **Anticipated airflow pattern: C**
4		1x Belong BF1212025MB2M 120 mm · 120 mm · 25 mm Reversible spinning direction **Anticipated airflow pattern: Alternating between B and C with direction change**
5		2x Belong BF1212025MB2M 120 mm · 120 mm · 25 mm Reversible spinning direction **Anticipated airflow pattern: Alternating between B and C with direction change**
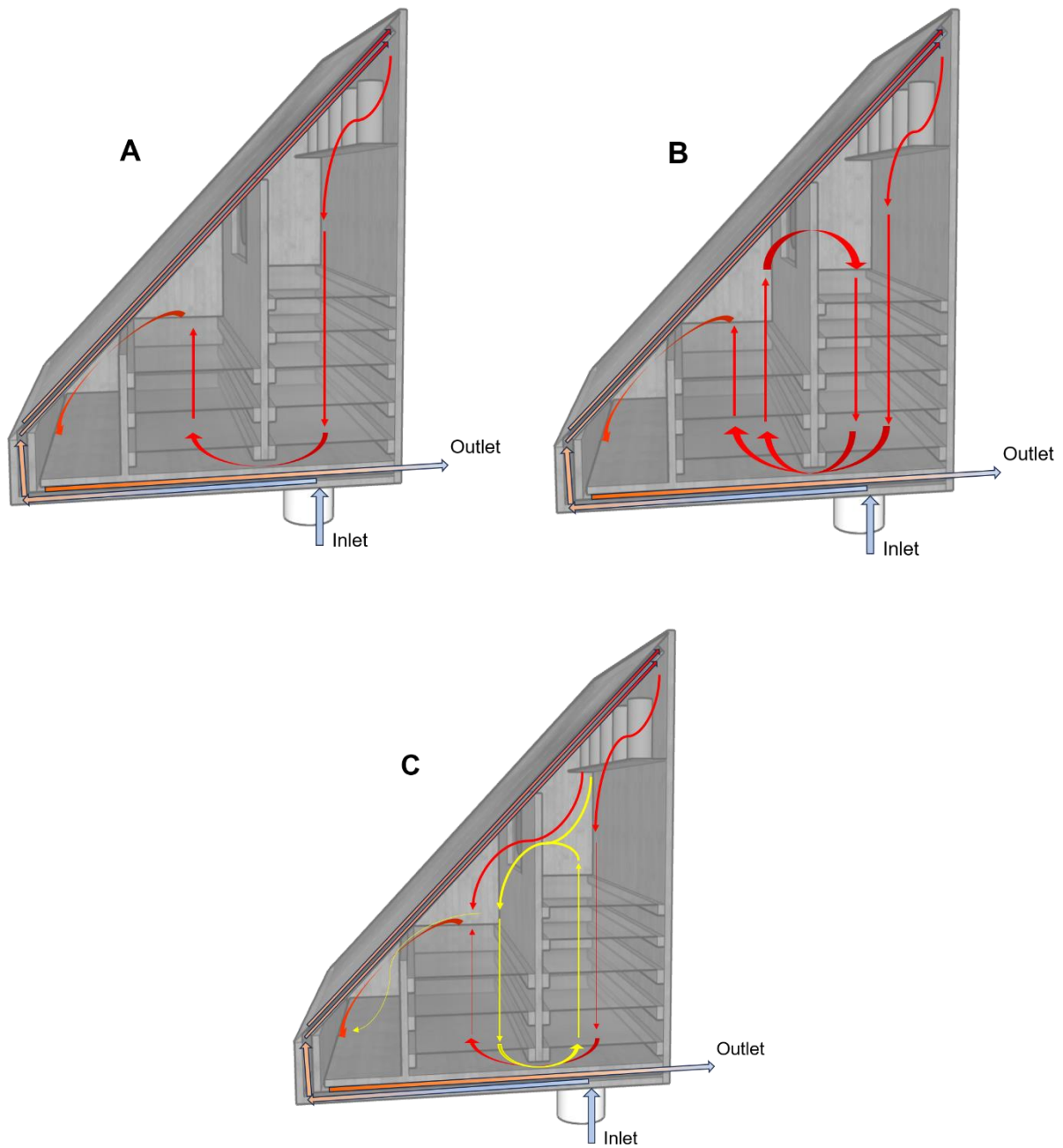
Figure 3-8: Anticipated airflow patterns for different fan setups

3.3   Measurement Plan

The initially set up measurement plan commenced with several test measurements to verify functionality of components and equipment. It is important to vary only one parameter at a time. Otherwise, it is difficult to identify the cause for certain outcomes. Table 3-4 below presents variable parameters as well as those that are unswayable due to given weather conditions or

external causes. The only parameter that was kept constant during all experiments was the internal and external fan's voltage.

Table 3-4: Variables and given external parameters during experiments

Constants	Variables	Given parameters

- Fan voltage of 12 V	- Quantity of food to be dried
	- Condition of food to be dried (thickness, pretreatments, etc.)
	- Number of trays inside dryer
	- Internal fan module
	- Heat storage
	- Number of weight measurements throughout the experiment
	- Drying time
		- Weather
		  ▪ Solar irradiance/ Cloud coverage
		  ▪ Temperature
		  ▪ Humidity
		  ▪ Wind
		- Sun's altitude
		- Maturity level of food to be dried

The drafted measurement plan was intended to be used as a living document adjusted at any point in time with new circumstances and discoveries.

The first experiments were conducted without heat storage. It was added at a later point in time.

The main difference between the measurements was the variation of the internal fan setup. The external fan's voltage was kept constant at maximum rated voltage of $12\,\text{V}$ which resulted in an inlet airflow of $21\frac{\text{l}}{\text{s}}$.

In order to obtain base case data to compare all following results to, the first experiments were conducted with no internal fan at all (Setup No. 1 – refer to Table 3-3 for overview of fan setups). Hence the hole in the big partition was completely covered.

After that, the same fan that had been used for experiments conducted with the improved dryer in Lund as well as in the previous model, was placed inside the dryer. First, spinning in the same direction as in previous experiments (Setup No. 2), then, spinning backward (Setup No. 3).

Banana drying experiments were limited to these three setups.

For the case of chili drying, one smaller reversible fan was utilized with change of flow direction every minute (Setup No. 4). Finally, the module with two of the same small reversible fans was placed in the dryer with the same setting (Setup No. 5). Due to lack of time, no experiments with the big fan spinning backward (Setup No. 3) were conducted during chili drying.

In order to compare the improved dryer's performance with the previous design, several

experiments were conducted using both dryers in parallel. During these experiments, the amount of produce inside the old dryer was adjusted according to absorber size to receive comparable data.

In the last step, multiple-day experiments were conducted utilizing heat storage overnight. As explained in Chapter 2.2.1, chilies must contain no more than 12 % moisture to be safe for storage, a condition that can require over 70 hours of drying. Given the goal of comparing different drying setups and the limited time available, chili drying experiments were not conducted with the intention of achieving this specific moisture level. However, to ensure that the drying process aligns with trends presented in literature, one three-day and one four-day experiment were carried out.

As this is an iterative process, several experimental setups were repeated due to weather conditions and to get additional data. It was initially planned to dry only banana but due to unforeseen circumstances, explained in Chapter 4.3, the produce was changed to small green chili.

3.3.1 Data Collection and Analysis

Every morning commenced with weighing each empty tray. During the first weeks, the respective quantity of bananas was peeled and sliced with a mandoline slicer. The slices were weighed and evenly spread on each tray.

After changing from drying bananas to drying chili, these were washed and dried the evening before. In the morning, the required quantity of small green chili was weighed and placed on the trays. For both cases, trays were put inside the solar dryer, internal and external fans were turned on and data collection commenced at 8:00 by activating the data logger measuring temperatures, relative humidities and solar irradiance.

According to Table 3-4 different variables were changed for different experiments but always just one at a time. Only for weight measurements during the experiment, the dryer's door had to be opened. Bananas were weighed with trays and chilies were weighed without trays. Inlet flow measurements were conducted several times on different days to verify a steady rate.

The last measurement was done at 17:00 or 18:00 each day. During daytime experiments, the fans and measurement equipment were turned off afterward. Only during over night drying experiments, the fans kept running and data got collected. At the end of each experiment, all measurements were downloaded from the data logger. The trays were cleaned and prepared for the next day.

In order to ease the analysis of each individual experiment, a program including several macros was written using Visual Basic for Applications in Excel. Weight measurements were analyzed individually as the number of measurements changed throughout the course of work.

To be able to calculate the drying rate, an average surface area for bananas and chili was determined. This was done by randomly selecting six bananas (= 700 g) and 116 chilies (= 300 g). The bananas' diameters and thicknesses were measured to calculate surface area. Chilies were measured in length as well as root diameter.

The last chili drying experiments were conducted with an installed heat storage comprising of ten 500 ml plastic water bottles. They were placed right below the absorber outlet at the inlet of the drying chamber (see Figure 3-9 below) in the morning of the first drying day.

Figure 3-9: Heat storage inside dryer

3.3.2 Open-Air Drying

As previously explained, open-air drying is currently the most common way of drying food in Bhutan. Farmers place their produce on roofs or other surfaces exposed to the sun's irradiance. To compare the obtained results with the outcome of this drying technique, several open-air drying experiments were performed in parallel to measurements with the solar dryer (see Figure 3-10 below). With this setup, it could be ensured that parameters, such as weather conditions on that specific day were exactly the same. Weight measurements were conducted at the same time and in the same way as for the trays inside the solar dryers.
Open-air drying experiments were conducted unshaded, shaded and with a commercial fan placed in front of the tray.

Figure 3-10: Open-air drying experiment with banana slices

4 Results

4.1 Data Verification

In order to verify functionality of the installed thermocouples, temperature measurements from those placed redundantly in close proximity were compared. In addition to 27 thermocouples, four relative humidity sensors also measured temperatures in four locations. Figure 4-1 and Figure 4-2 show plots of measurements at the inlet and chamber 1 over two days for illustration. As there are only very minor deviations, functionality could be verified.
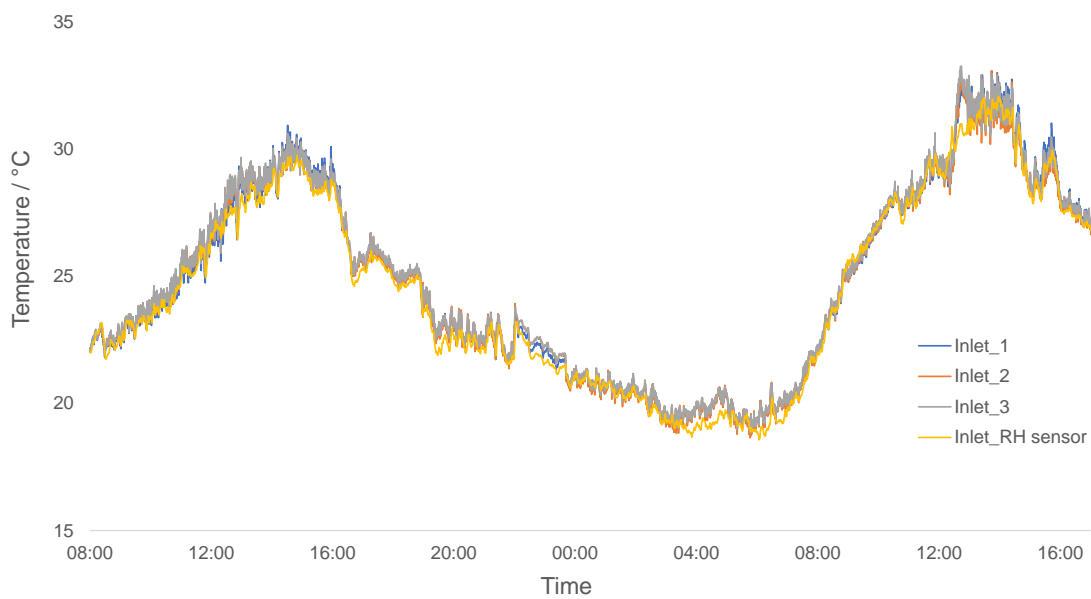
Figure 4-1: Inlet temperature measurements from thermocouples and relative humidity sensor
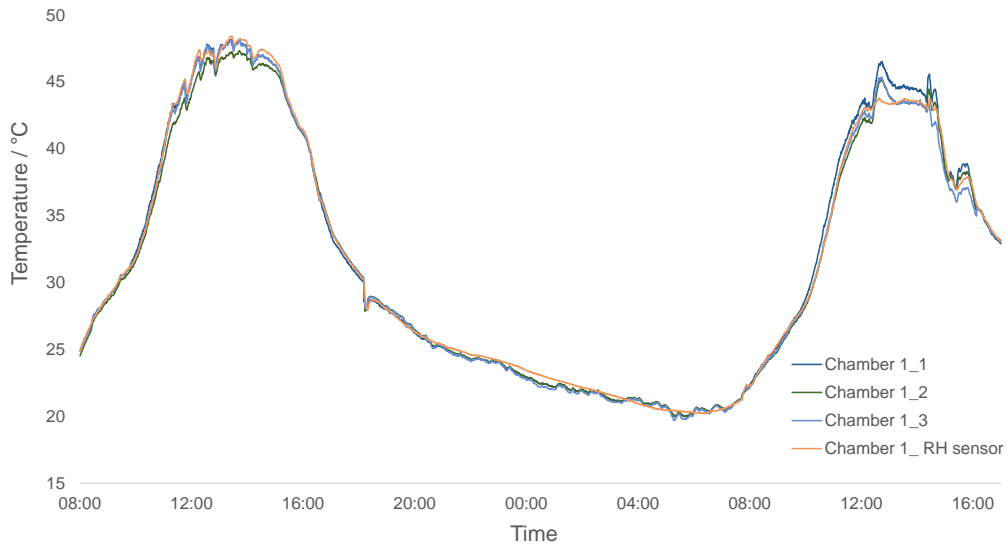
Figure 4-2: Chamber 1 temperature measurements from thermocouples and relative humidity sensor

Verification of solar irradiance measurements revealed that the collected data from the pyranometer was off by a factor of 1.5. This was discovered by comparing the measured values to those of a local weather station and in addition to readings from a hand-held Frederiksen 4890.2 pyranometer. Figure 4-3 shows the original values measured by the CMP3 pyranometer, as well as data from the local weather station for that same day. The deviation was adjusted by multiplying all pyranometer data points with the obtained factor resulting in the adjusted curve plotted below.
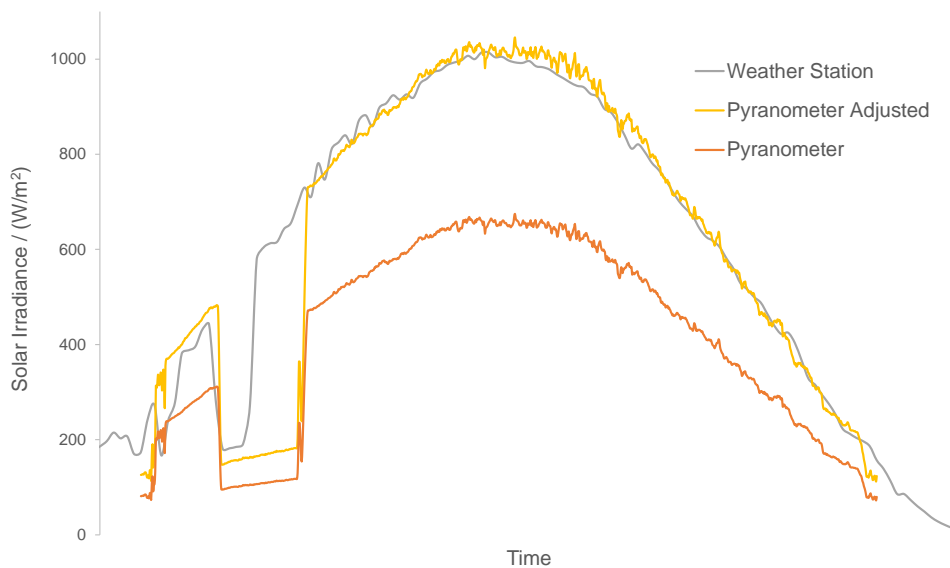
Figure 4-3: Solar irradiance measurements from pyranometer and weather station on March 17

4.2 Solar Irradiance and Temperature Variations

Table 3-4 presents given parameters that could not be influenced. While e.g. wind speed and direction were not assessed, ambient temperatures and solar irradiance were measured throughout the experiments. The following Figure 4-4 and Figure 4-5, show solar irradiance and ambient temperature plots from different days to highlight how significant the differences were, even though the experiments were conducted within a timeframe of two months (March – April 2024). It needs to be noted that in Figure 4-5 the graph's ordinate is broken at 15 °C.
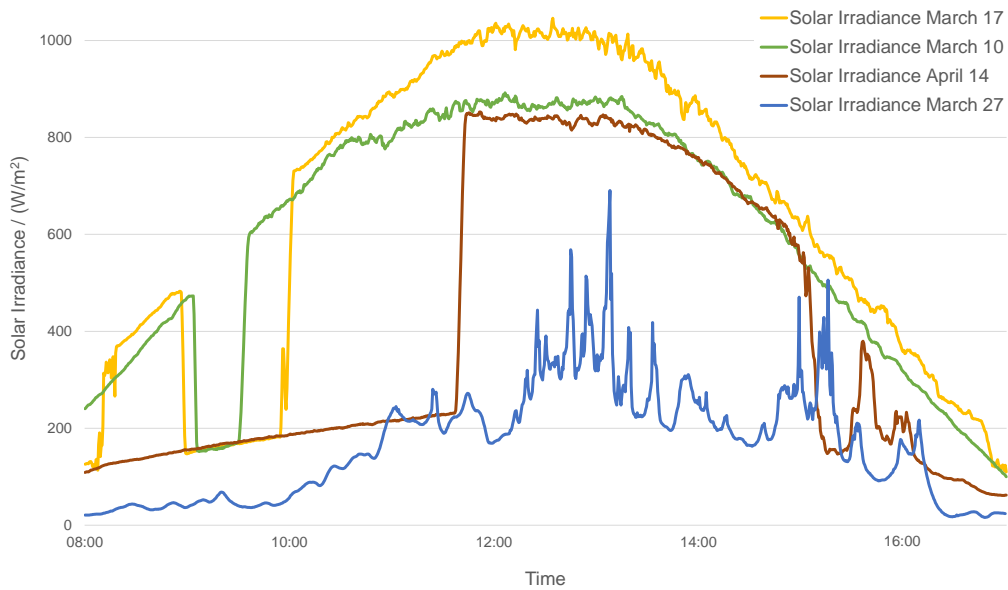
Figure 4-4: Solar irradiance measurements for different days with different weather conditions
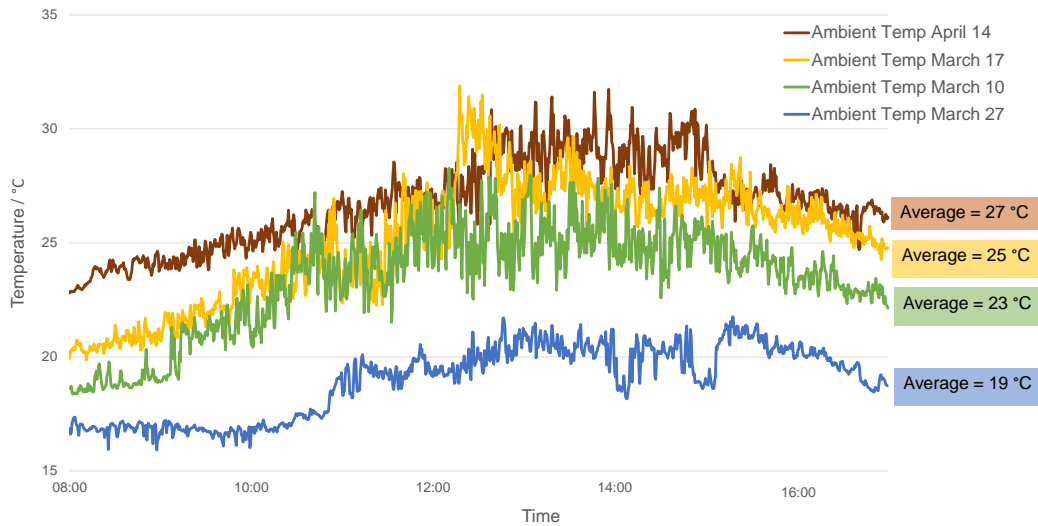
Figure 4-5: Ambient temperature measurements for different days with different weather conditions

The plots not only show the difference between warm sunny days (March 10, 17 and April 14) and colder cloudy days (March 27) but also point out another circumstance. The solar dryer was placed close to a building in order to be able to store measurement equipment inside. Although the absorber was facing south and there was no big roof overhang, there was still shading caused by the house's roof. At the beginning of the experiments (March) it shaded the dryer for approximately 25 minutes from around 9:00 to 9:25. This shaded time increased to almost four hours by the last day of experimenting (8:00 to 12:00).

Another observation is that higher solar irradiance does not directly relate to higher temperatures. Although March 17 recorded the highest solar irradiance values in this comparison, the ambient temperatures on April 14 were higher.

4.3   Banana Drying

4.3.1   Comparison of different Banana Drying Setups

During the experiments, bananas were sliced into $2\,\text{mm}$, and $150\,\text{g}$ were placed on each of five trays. The drying time was initially limited to one day (9 hours) with hourly weight measurements. This arrangement was chosen as a starting point with the possibility to adjust the amount of bananas per tray, number of trays (maximum of eight), drying time and frequency of weight measurements. The following Figure 4-6 shows plots for three different fan setups: No fan (Setup No. 1 - refer to Table 3-3 for overview of fan setups), big fan spinning forward (Setup No. 2) and big fan spinning backward (Setup No. 3). In addition, shaded and unshaded open-air drying was performed. The curves for the different fan setups were generated by averaging the weight of all five trays.

For reference, Figure 4-7 presents solar irradiance and ambient temperature during each of the experiments. The graph's secondary ordinate is broken at 17 °C.
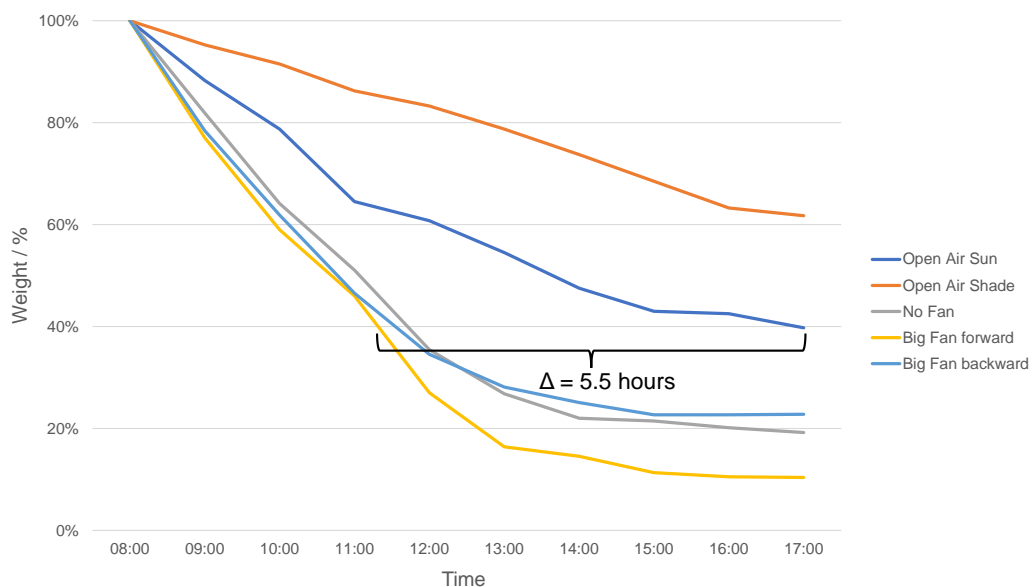
Figure 4-6: Comparison of different fan setups (average of 5 trays with 150 g banana slices each) and open-air drying of banana slices
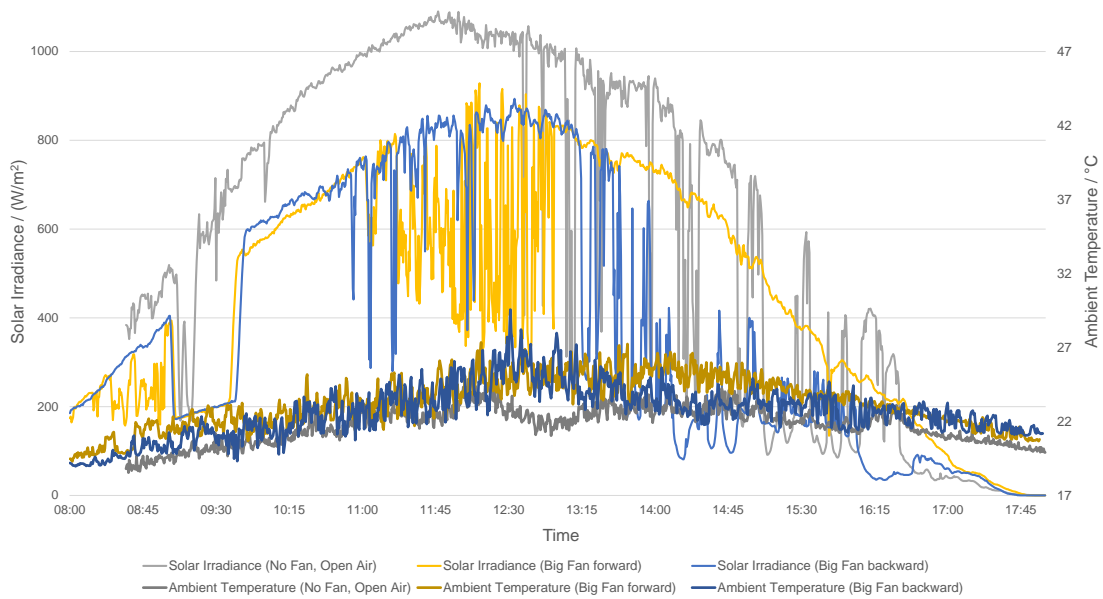
Figure 4-7: Solar irradiance and ambient temperature during banana drying experiments

The plots in Figure 4-6 display weight reduction during each of the setups and open-air drying. Operating the dryer with the big internal fan spinning forward (Setup No. 2) led to the highest moisture removal after 9 hours of drying, and shaded open-air drying to the lowest. In order to reach 40 % of the initial weight, it saves 5.5 hours to use the solar dryer with the big fan spinning forward (Setup No. 2) in comparison to unshaded open-air drying.

Ambient temperatures were similar during all experiments with an average of 22 °C for the first experiment without internal fan and 23 °C for the experiments with big fans. However, solar irradiance was noticeably higher during the first experiments (without any internal fan and open-air) as plotted in Figure 4-7.

Figure 4-8 shows photos of the dried banana slices.

Figure 4-8: Dried banana after nine hours with fan Setup No. 2

Evenness of Banana Drying in Different Setups

The previous graphs presented an overview with averaged results from all trays inside the solar dryer. Plots in Figure 4-9 below visualize the differences in drying rate between the individual trays inside the dryer (refer to Figure 3-4 for numbering of trays). For better clarity, only the fastest and slowest dried trays are shown.
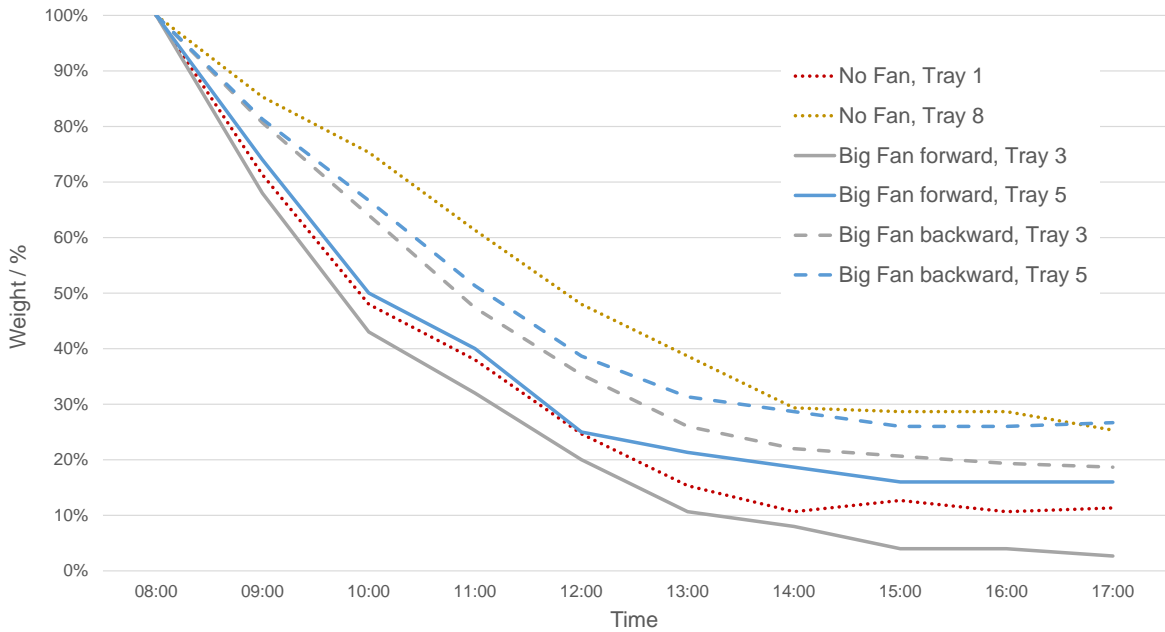
Figure 4-9: Drying curves of individual trays during banana drying in different fan setups

The graphs show how there was not only a difference in the uniformity of drying between the various trays, but also in which tray dried the fastest and which dried the slowest. During the first experiment without internal fan (Setup No. 1, dotted line), tray 1 (red) dried fastest and tray 8 (yellow) slowest. Refer to Figure 3-4 for tray arrangement inside dryer. For the second and third experiment with the big fan spinning forward and backward (Setup No. 2 and No.3 - refer to Table 3-3 for overview of fan setups) tray 3 (grey) dried fastest and tray 5 (blue) was slowest.

However, the most uniform drying pattern was achieved with the big fan spinning backward (Setup No. 3). In that case, the weight difference between the fastest drying tray 3 and the slowest drying tray 5 was at 8 % while it was 13 % for the big fan spinning forward (Setup No. 2).

Another result from comparing these different drying setups is that the curves flatten around 15:00 in the afternoon and the banana slices dry much slower or even regain weight in some cases.

4.3.2 Multiple-Day Banana Drying Experiments

The next experiment was conducted over the course of two days. It included parallel measurements with the previous dryer design and unshaded open-air drying with and without a commercial fan for comparison. As the previous dryer design incorporates a fixed fan Setup No. 2 (refer to Table 3-3 for overview of fan setups), the same was chosen for the improved dryer design in order to receive comparable data. Figure 4-10 below highlights the different weight reduction patterns for all setups.
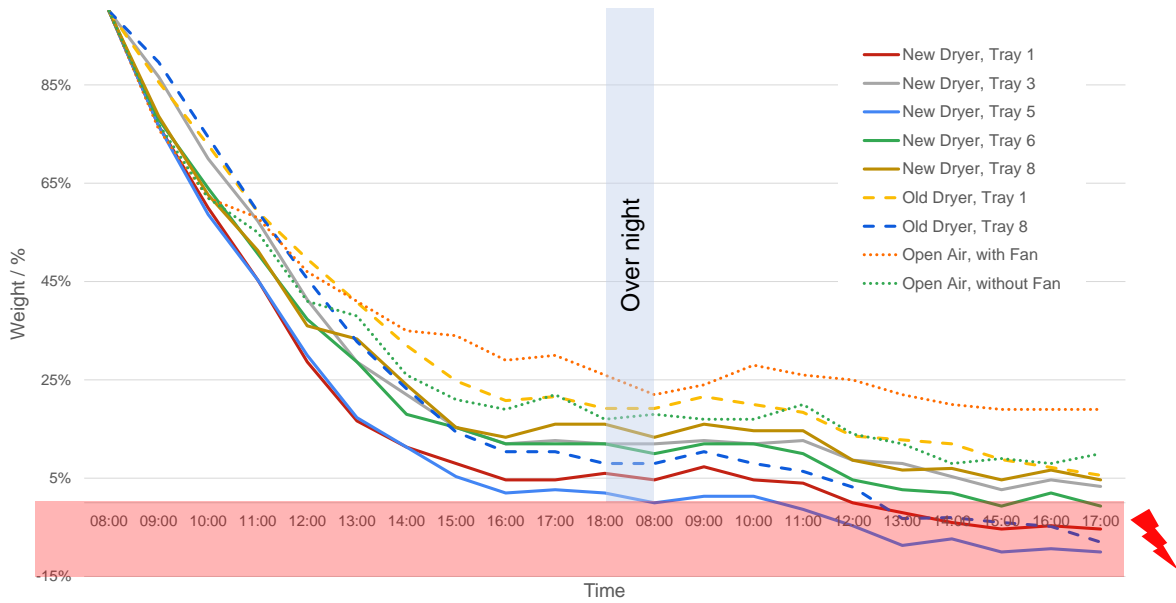
Figure 4-10: 2-day-experiment in comparison to previous dryer design and open-air drying

For this and following plots, the over night period represents 14 hours on the abscissa (18:00 – 08:00).

Similar to plots in Figure 4-6 open-air drying accounts for the lowest percentage of lost weight. It becomes apparent that especially during the second day of drying, the graphs are very unsteady and a striking error is clearly visible in these plots. They indicate that the weight of the bananas reaches negative values during the second day, which is clearly implausible.

The reason for this is that it was not possible to weigh the trays in the beginning of the second day and therefore the tray weight measurements from the first day were used to calculate the banana's weight. As these clearly deviate, an additional experiment was conducted during which only the empty trays were placed inside the dryer and weighed every hour (see Figure 4-11 below).
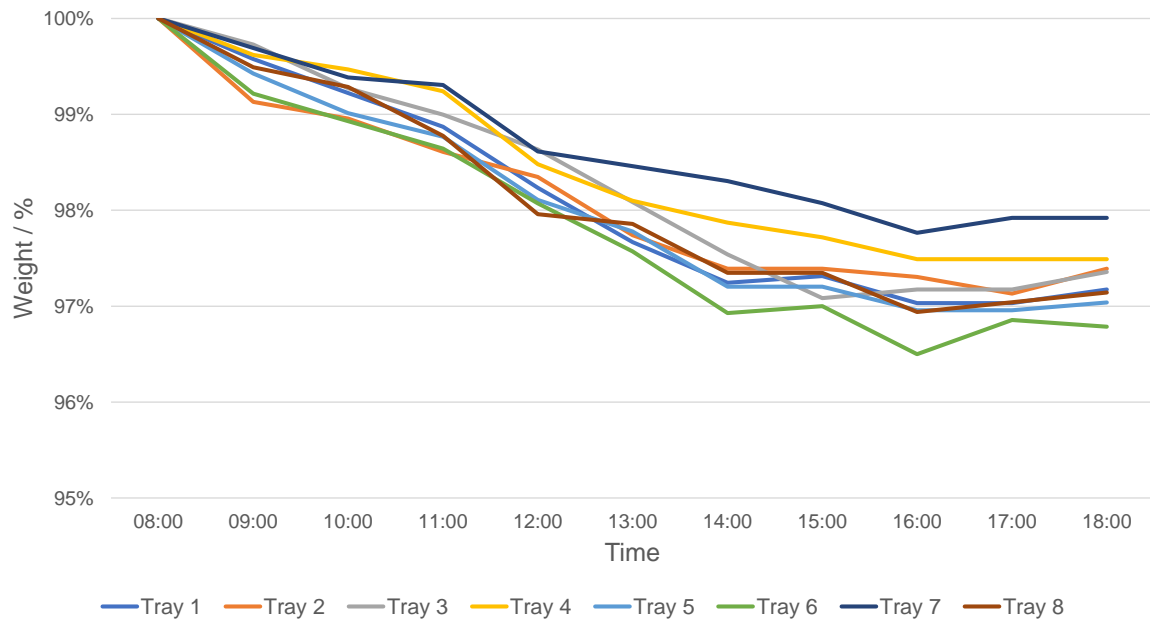
Figure 4-11: Weight measurements of drying only empty trays

The plot visualizes the unevenness of the drying process of each individual tray (note that the graph's ordinate is broken at 95 %). They not only dry at different rates but also non-linearly which makes it impossible to anticipate how much weight the trays themselves lose during the drying process. Considering absolute values, the greatest weight reduction occurred at tray 6 with $49\,\text{g}$ difference. Taking into account that the weight of banana slices per tray had been equal to $150\,\text{g}$, this has a significant influence. The matter will be further discussed in Chapter 5.1. This circumstance ultimately led to the decision to change the produce to be dried in the following experiments.

The issue originated from the fact trays had to be weighed along with the banana slices during measurements. Consequently, the objective became finding a product that could be weighed independently of the trays. After thorough consideration, the decision was made to use small green chili. Chilies are not only easier to weigh separately but are also one of the most popular and common produce and cash crops in Bhutan.

4.4 Chili Drying

4.4.1 Comparison of different Chili Drying Setups

Initially, $300\,\text{g}$ small green chilies were placed on each of five trays. The drying time was two days ($2 \cdot 10$ hours) with three weight measurements. The following Figure 4-12 shows plots for four fan

setups (refer to Table 3-3 for overview of fan setups) and unshaded open-air drying. The curves for the different fan setups were generated by averaging the weight of all five trays during different experiments taking different weather scenarios into consideration.
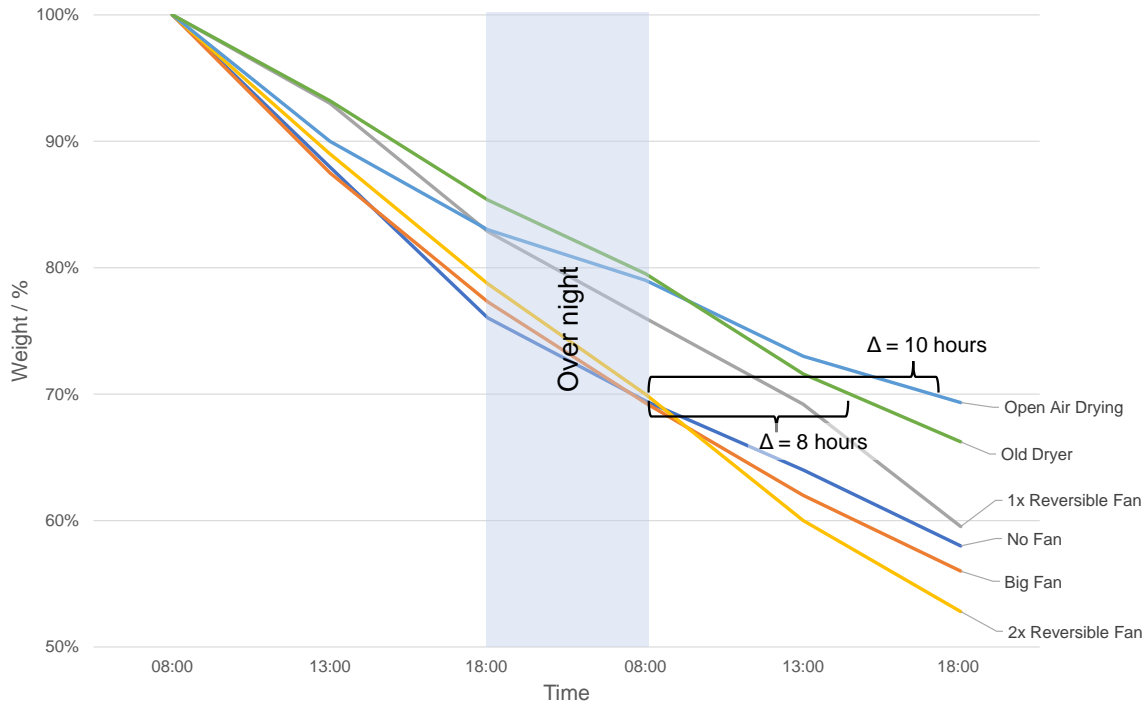
Figure 4-12: Comparison of different fan setups (average of 5 trays with 300 g chili each), drying in the previous dryer design and open-air drying of chili

The plots display weight reduction during each of the two-day experiments. It needs to be noted that the graph's ordinate is broken at 50 % weight. In all setups, the drying curve follows a linear trend during the daytime. Chilies dried slowest during open-air drying and experiments with the previous dryer design. In order to reach 70 % of the initial weight, using the improved design saved 8 hours compared to the previous design and 10 hours compared to unshaded open-air drying.

Comparing different setups in the improved dryer design revealed that utilizing two of the reversible fans (Setup No. 5) led to the highest weight reduction after two days. It is followed by having the big fan spin forward (Setup No. 2), using no fan at all (Setup No. 1) and lastly using one reversible fan (Setup No. 4).

Evenness of Chili Drying in different Setups

Drying curves of all chili drying experiments followed a linear trend as illustrated in Figure 4-12. The relevant difference lies in the drying rate and final weight reduction of the produce which represents evenness among the trays. Figure 4-13 below shows the differences in final weight among each tray for the different fan setups.
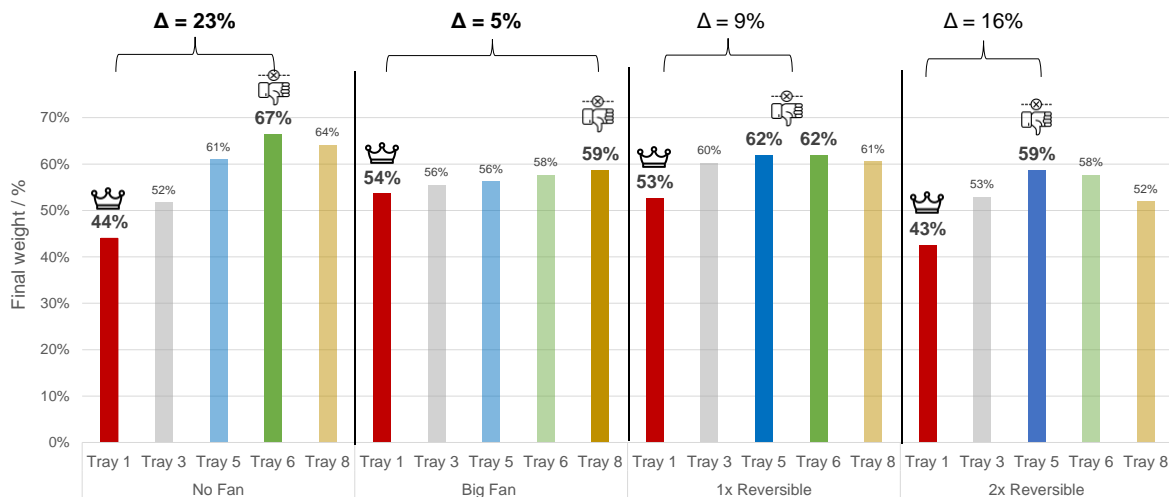
Figure 4-13: Final weights of chilies after drying for two days with different fan setups highlighting the trays with lowest and highest weights

Throughout the experiments, chilies on tray 1 (red bars) lost the highest amount of weight (refer to Figure 3-4 for tray arrangement inside dryer). Bars and icons in Figure 4-13 show how for different setups, different trays lost the least amount of weight. As previously mentioned, drying with two reversible fans (Setup No. 5) led to the highest weight reduction but the most even drying result was achieved by utilizing the big fan (Setup No. 2) with 5 unit % weight difference between the best and worst tray. Using no fan (Setup No. 1) at all resulted in the highest deviance with 23 unit %.

Chili Storage and Drying over night

As all chili drying experiments were conducted for at least two days, trays with chilies were stored or dried over night. Table 4-1 below presents different options and the respective percentage of weight loss encountered during night.

Table 4-1: Weight reduction through different chili storage and drying scenarios over night

Location of trays		Internal fan		Heat storage		Weight reduction over night
Inside Dryer	Outside Dryer (in sealed black plastic bags)	Turned on	Turned off	Yes	No	
	✓					7 %
✓			✓		✓	6 %
✓		✓			✓	6 %
✓		✓		✓		5 %

The weight reduction for all four scenarios is very similar with a maximum deviation of 2 %. Storing the trays outside of the dryer in sealed plastic bags led to the highest weight reduction. Letting the dryer run over night with installed heat storage resulted in the lowest drying performance.

4.4.2 Chili Drying; increased Quantity and extended Drying Time

There were two possible ways of increasing chili quantity: Increasing the amount of chilies per tray and the number of trays.

The following Figure 4-14 visualizes weight differences due to an increased amount of chili per tray ($500\,g$ instead of $300\,g$). The results are based on combined data from four different experiments utilizing reversible fans (Setups No. 4 and No. 5 - refer to Table 3-3 for overview of fan setups). The data was merged to consider a broader range of external circumstances. Note that the graph's ordinate is broken at 50 %.
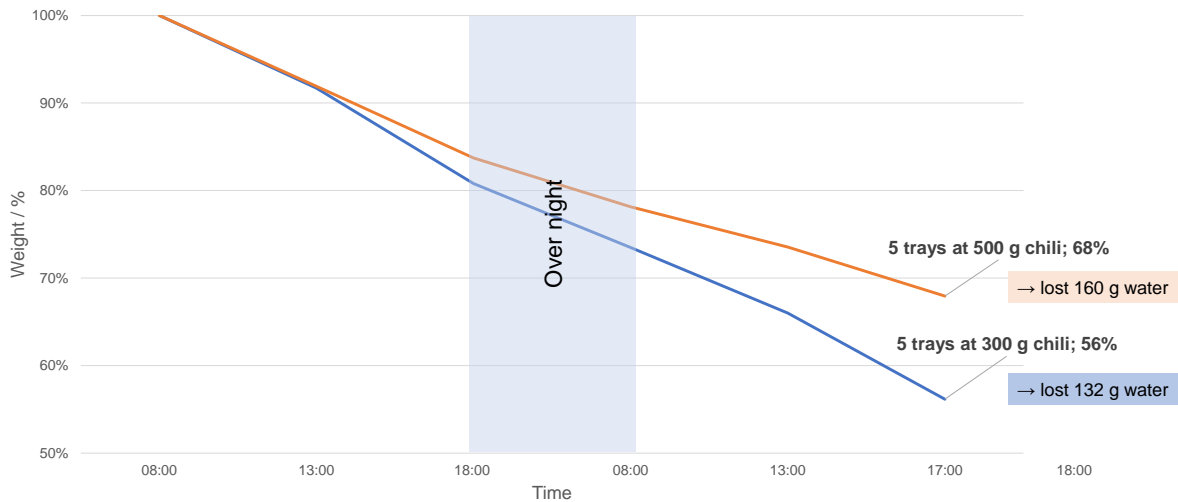
Figure 4-14: Difference in weight reduction of drying 5 trays with 300 g and 500 g of chili; combined data from multiple experiments

Increasing the amount of chili per tray by 67 % (from 300 g to 500 g) in average led to a decrease in relative drying performance of 12 % (from 56 % to 68 %). In the 300 g experiment, 132 g of water were reduced and in the 500 g experiment, 160 g (difference of 19 %).

In the second scenario, the number of trays inside the dryer was increased from five to the maximum of eight trays. In this case, the results are merged from multiple experiments with the big fan spinning forward (Setup No. 2).
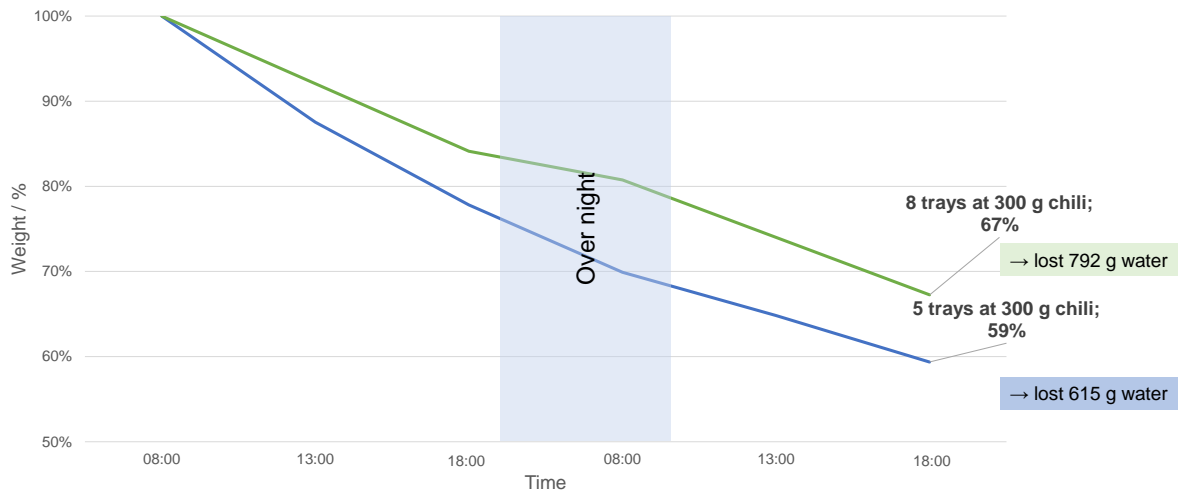
Figure 4-15: Difference in weight reduction of drying 5 trays with 300 g and 8 trays with 300 g of chili; combined data from multiple experiments

Increasing the number of trays by 63 % (from 5 to 8) led to a decrease in drying performance of 8 % (from 59 % to 67 %). In the experiment with 5 trays, $615\,\mathrm{g}$ of water were reduced and with 8 trays, $792\,\mathrm{g}$ (difference of 22 %).

Finally, one three-day and one four-day experiment were conducted to verify the continuous linear trend seen in previous drying curves. Since fan Setup No. 5 (two reversible fans) delivered the most promising results, it was selected for the multi-day experiments. Results from the four-day experiment are presented in Figure 4-16 below. For completeness, the following graph contains not only percentaged weight reduction during the drying process, but also the respective drying rates in $^{\mathrm{g}}/_{\mathrm{h}\,\cdot\,\mathrm{m}^2}$ calculated according to Eq. 2.3. Yellow bars represent the averaged drying rate during the day and the blue bars during night with installed heat storage. Note that the graph's ordinate is broken at 20 %.
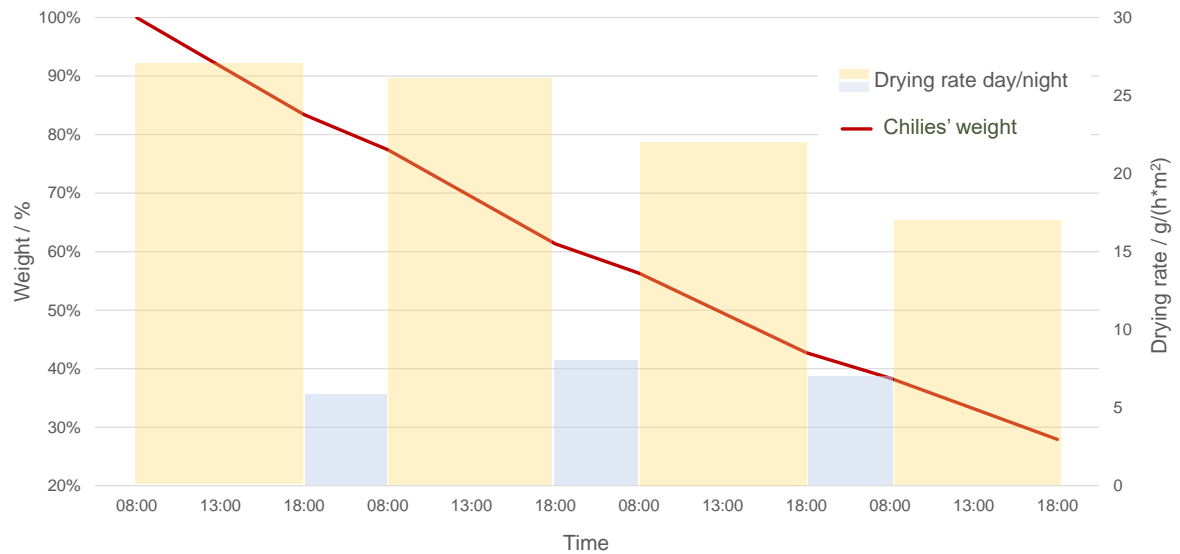
Figure 4-16: Drying processes during 4-day experiment showing weight reduction and drying rate utilizing two reversible fans and heat storage

During each day, the drying curve has a nearly linear trend. It needs to be taken into account that the time for daytime measurements is 10 hours (08:00 - 18:00), while the nights account for 14 hours (18:00 - 08:00). The coefficient of determination $R^2 = 0.99$ which means that 99% of the variance in the measured values (only during daytime) can be explained by the independent variable using a linear model.

The yellow bars indicate how the drying rate is declining each day of the experiment which is also due to weather conditions. While the maximum solar irradiance was at $899\frac{W}{m^2}$ on the first day, its peak reached only $742\frac{W}{m^2}$ on the last day.

It becomes apparent that the drying rate is significantly lower during night even though the heat storage was installed. The following Figure 4-17 shows photos of the dried chilies after four days.

Figure 4-17: Dried chili after four days with fan Setup No. 5

4.5   Components' Performances

4.5.1   Heat Exchanger

Figure 4-18 below shows the heat exchanger's efficiencies (calculated according to Eq. 2.10 and Eq. 2.11) as well as the temperature ratio which is used to calculate the dryer's leakage following Eq. 2.12. The temperature differences on each side of the heat exchanger are plotted for the same day (see Figure 4-19). The plots were chosen as a representation of typical measurements throughout an average day (average solar irradiance and ambient temperature). The data was collected during a chili drying experiment and the dryer remained closed throughout the day.
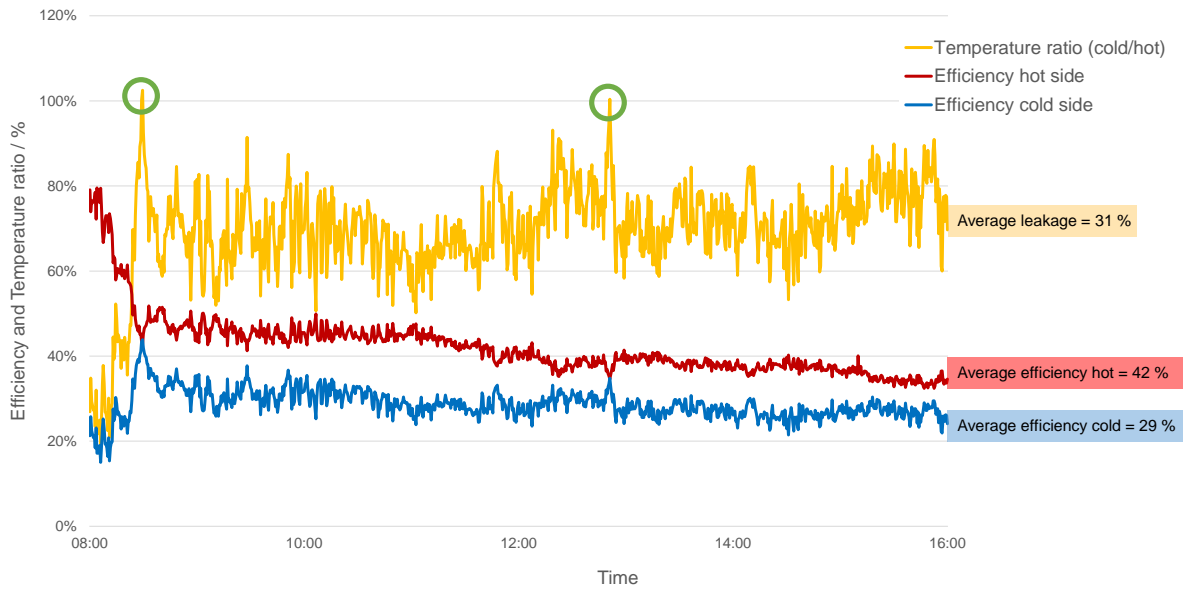
Figure 4-18: Heat exchanger efficiencies and mass flow leakage during drying

The efficiencies were low during the first hour of operation and fluctuated slightly throughout the day. The average leakage was 31 %, while the average efficiencies were 29 % for the cold side and 42 % for the hot side.
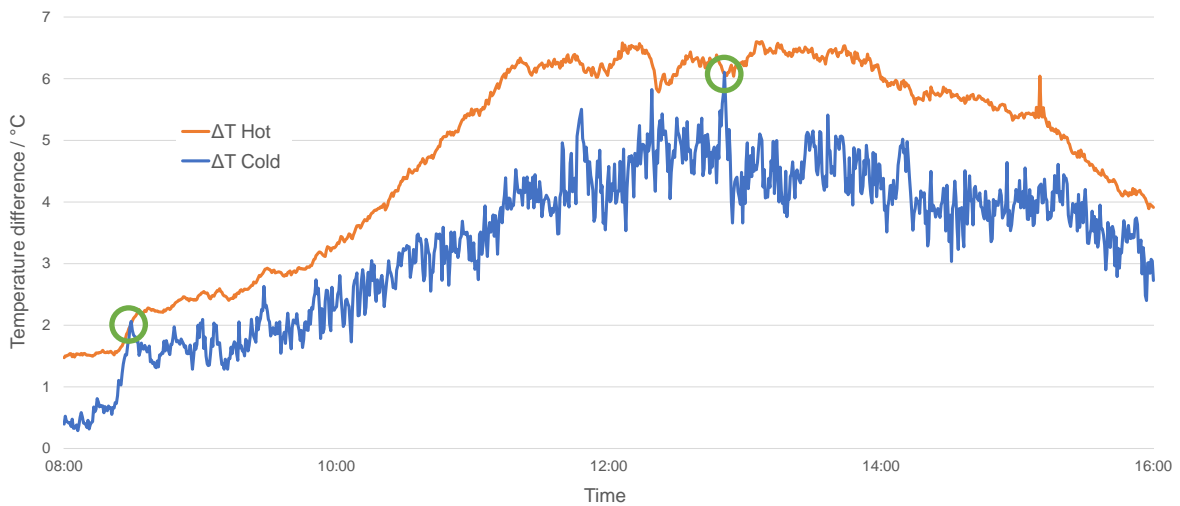
Figure 4-19: Temperature differences on each side of the heat exchanger

The temperature differences on the hot and cold heat exchanger side rise until midday, stay rather constant for a few hours to then decrease. At some points during the day, the difference on each side is exactly the same which leads to an efficiency of 100 % marked with green circles in Figure 4-18 and Figure 4-19.

4.5.2 Absorber

The absorber efficiency was calculated according to Eq. 2.13. Figure 4-20 below highlights its relation to solar irradiance and Figure 4-21 presents the absolute temperature differences between absorber in- and outlet. This data was collected on a sunny day with low cloud coverage representing good external conditions for operating the solar dryer (refer to Figure 4-4 for examples of less ideal conditions).
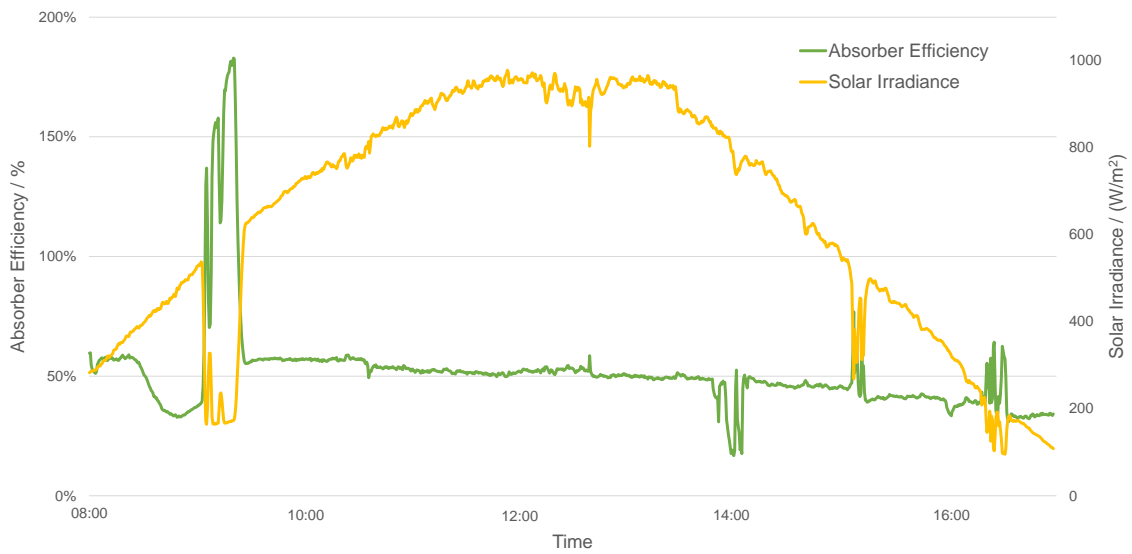
Figure 4-20: Absorber efficiency and solar irradiance correlation
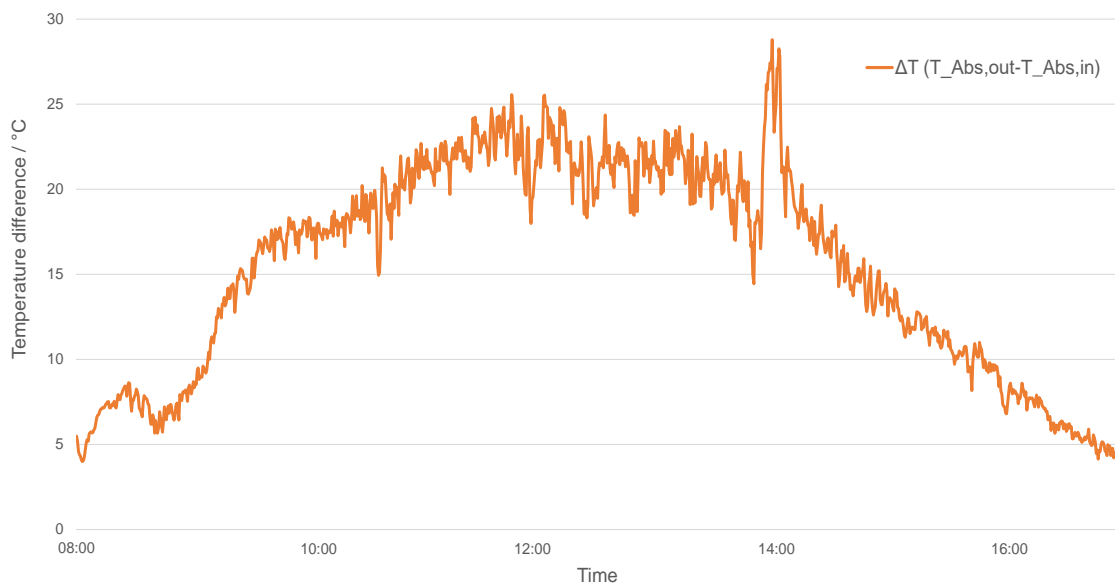
Figure 4-21: Absolute temperature difference between absorber in- and outlet

The absorber's efficiency exceeds 50 % even at the start of the experiments in the morning, just after turning on the fans. The temperature difference between in- and outlet is already at 5 °C at this point. Efficiency drops and then rises above 100 % during the phase in which the dryer is shaded by the house corner (see Chapter 4.2 for more details). Referring to Eq. 2.13 reveals that the reason for this is the sudden drop in the maximum possible heat transfer rate (denominator) due to the shade. Since the temperatures at the absorber do not drop that abruptly, the numerator and therefore the value for $\eta_{Absorber}$ can exceed 100 % during this period. Afterward, the graph follows a linear trend with efficiencies around 50 %.

The maximum temperature difference reaches 28 °C.

4.5.3 Drying Chamber

Multiple thermocouples were located inside the drying chambers (see Figure 3-7). Figure 4-22 below illustrates average (circular markers) and maximum (triangular markers) temperatures at each chamber during different fan setups. Note that the graph's ordinate is broken at 30 °C. Average temperatures were calculated over entire one-day experiments, with peak values occurring between 12:00 and 13:30.
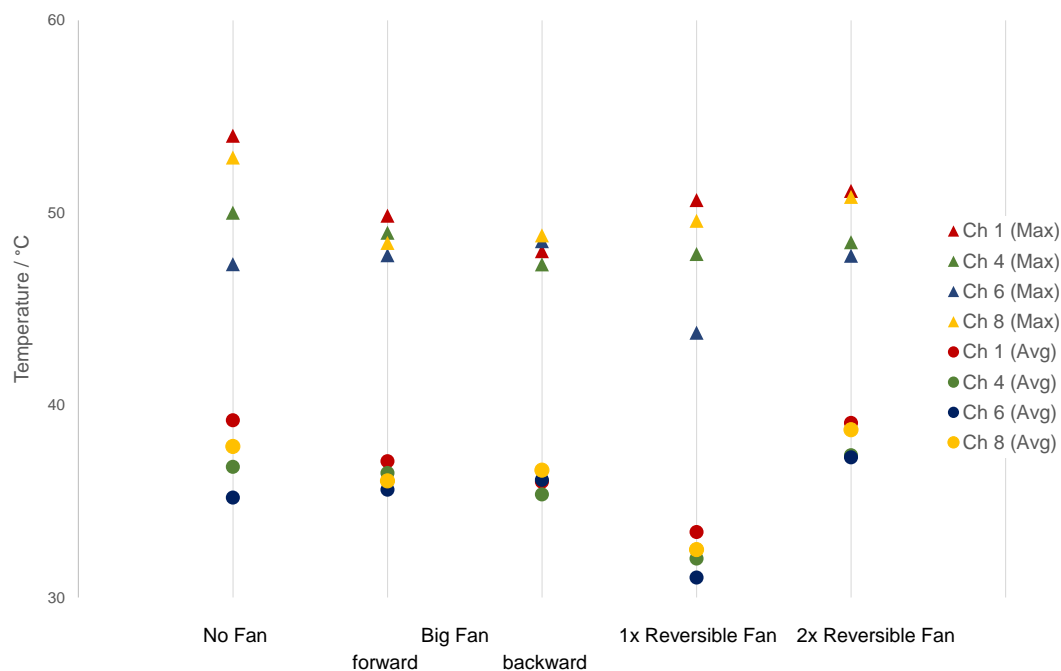
Figure 4-22: Temperature profile inside the drying chambers showing average and maximum temperatures for different fan setups

The plot very clearly shows how different fan setups influence the temperature profile inside the dryer. In this case, the focus should be on relative differences rather than absolute temperature

values as these are strongly dependent on the weather on each specific day.

Chamber 1 records the highest temperatures in every setup except for the big fan spinning backward (Setup No. 3 - refer to Table 3-3 for overview of fan setups). Using no fan (Setup No. 1) leads to a clear order from highest to lowest temperature. As there is no active circulation inside the dryer, chambers 1 and 8, located closest to the absorber, achieve the highest temperatures. Utilization of the big fans (Setup No. 2 and No. 3) leads to lower differences in average temperatures between each chamber. When using two reversible fans (Setup No. 5), chambers 1 and 8 as well as 4 and 6 record similar average temperatures but the difference between both pairs is visible.

4.5.4   Heat Storage

The last chili drying experiments were conducted with installed heat storage (see Figure 3-9). Figure 4-23 below displays the temperatures at absorber outlet, inside the heat storage (water bottles) and on the outside of the heat storage during a three-day-experiment. Note that the graph's ordinate is broken at 15 °C.
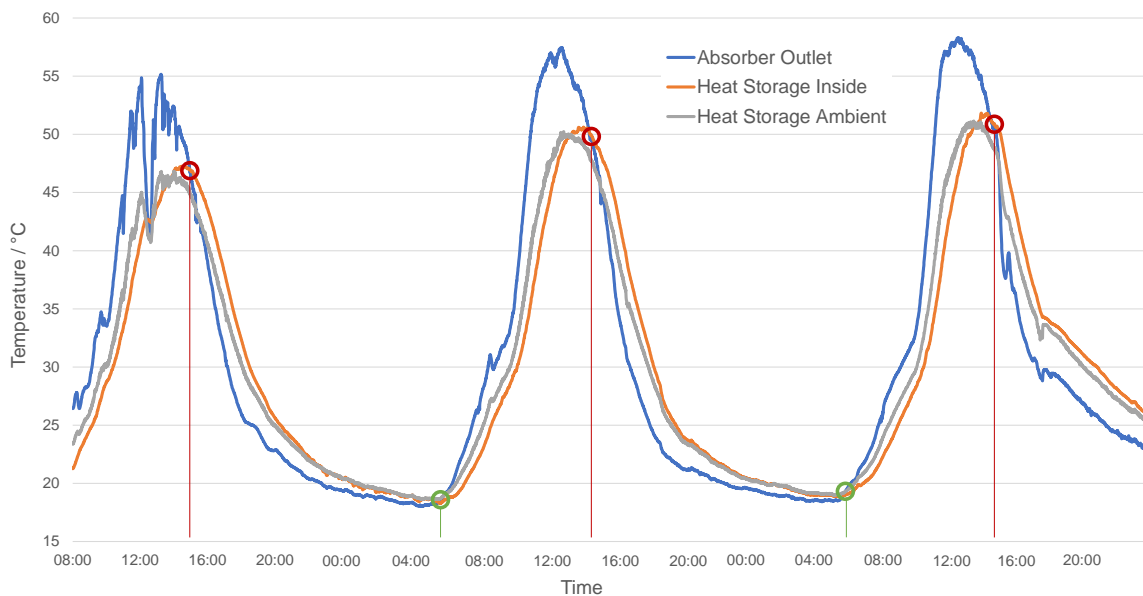
Figure 4-23: Temperature at heat storage and absorber during a three-day-experiment

Intersections of the plots show that it takes until approximately 15:00 each day for the heat storage to absorb enough thermal energy to reach a higher temperature than the air leaving the absorber (red circles). From this time until around 6:00 the next morning, the heat storage maintains a higher temperature (green circles). Hence the heat storage needs nine hours to absorb enough energy to supply heat for the next 15 hours.

4.6   Humidity

Four humidity sensors were installed at the dryer (see Figure 3-7). They measure temperature and RH. In order to be able to compare values at all four positions, the AH values in $^g/_{m^3}$ were calculated according to Eq. 2.1. Figure 4-24 below presents a typical humidity profile on a rather warm and humid day (average temperature = 23 °C, average RH = 65 %). Note that the graph's ordinate is broken at $12\frac{g}{m^3}$.
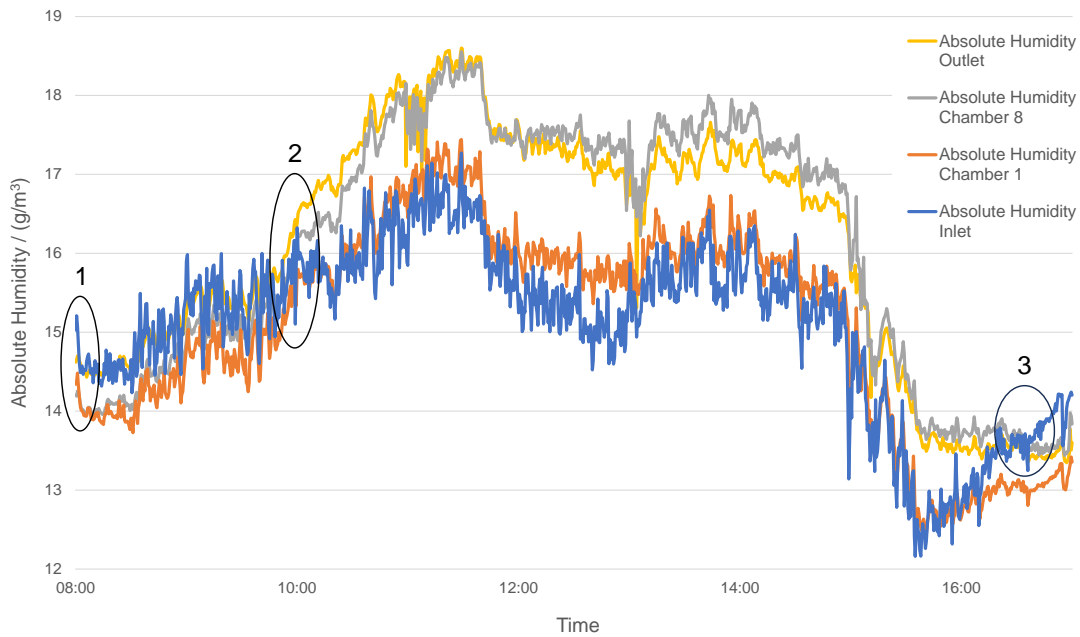
Figure 4-24: Absolute humidity measurements from four installed sensors at the dryer

In the beginning of the experiment, AH at inlet and outlet as well as chamber 1 and chamber 8 were fairly equal (1). After 10:00, AH levels in chamber 8 and at the outlet rise significantly as the drying process intensifies, and moisture from the produce inside the dryer is picked up by the airflow (2). The graph declines in the afternoon and during sundown, inlet humidity exceeds all other values (3).

Plotting RH measurements in relation to different fan setups, as done for temperature recordings (see Figure 4-22), did not reveal any significant correlations. Consequently, average RH values for all experiments were calculated, ranging between 33 % and 35 %.

5 Discussion

5.1 Banana and Chili Drying Characteristics

Banana Drying

Initial banana drying experiments showed that the moisture content threshold to be safe for storage can be achieved within one day of drying. Among the compared fan setups, the shortest drying time and highest moisture removal were achieved with the big fan spinning forward (Setup No. 2 - refer to Table 3-3 for overview of fan setups). The most uniform drying pattern was observed with the big fan spinning backward (Setup No. 3). An interesting observation is that the drying process seemed to stop for all trays at the same point in time as the drying curve flattens after approximately 15:00 (see Figure 4-6 and Figure 4-9). No reasonable explanation for this phenomenon could be found as it was expected for all trays to dry to the same weight level eventually.

Although the banana drying experiments seemed to bear promising results at first, unexpected challenges arose. One of the external and therefore given parameters as stated in Table 3-4 was the maturity level of bananas to be dried. During the first experiments, unripe green bananas with a firm texture were used. After drying, taking the bananas off the trays took some time but worked well. However, after just a few days, when the bananas would ripen further, it became very difficult to take them off the trays after drying. They would stick to the wire mesh on the trays (see Figure 5-1 below) and the only way to thoroughly clean the trays for the next experiments was to soak them with water which was not only very time-consuming but also led to another issue.

Figure 5-1: Leftovers of dried banana slices on trays during cleaning process

After cleaning the trays in the evening, they were stored to dry. However, when they were filled with banana slices and prepared for the next experiment the day after, they had not fully dried. As a result, not only the banana slices dried during the experiment, but so did the trays. Experiments drying only the trays were conducted but as shown in Figure 4-11, the drying was very uneven and practically impossible to predict. This in return led to unusable results as presented in Figure 4-10. Subtracting the initial weight of the, still wet, trays from hourly banana weighings finally resulted in negative values. Hence, it was not possible to reliably measure how much of the weight reduction (moisture removal) derived from bananas and how much from the trays.

Consequently, there was a need to change the produce to be dried. Chili was deemed suitable as it can be taken off the trays for weighing, did not stick to the trays and was available.

Chili Drying

Chilies dried significantly slower than bananas which is why it was necessary to extend drying experiments to a minimum of two days to get viable results. This extended drying time limited the number of different drying setups that could be tested.

During the conducted experiments, using two reversible fans (Setup No. 5 - refer to Table 3-3 for overview of fan setups) resulted in the highest weight reduction while the most uniform results were achieved with the big fan (Setup No. 2).

As the moisture content of the chilies decreased, the drying rate declined.

Increasing the amount of chili per tray and the number of trays both resulted in only slightly decreased drying performance. This leads to the choice of drying higher quantities in a slightly extended drying time or accelerating the drying process by filling the dryer with less produce.

Comparison of Drying Process: Bananas vs. Chilies

In general, weather conditions, especially solar irradiance, had a profound impact on drying efficiency, with higher irradiance leading to better drying performance. Suitable drying conditions (temperature and humidity values) were achieved, but optimal values could only be reached temporarily (see Figure 4-22). However, as literature suggested, sliced bananas dried much faster than uncut chili.

During the first five hours of all chili drying experiments, there was barely any difference in drying rate independent from weather or fan setup indicating that the drying processes needed a certain amount of time to commence. This is possibly due to the fact that chilies were uncut and kept their peel while bananas were cut open and therefore more exposed.

A big difference between bananas and chilies was the drying behavior over night. While bananas barely lost any weight or even reabsorbed moisture (see Figure 4-10), chilies continued to dry losing up to 7 % of weight. It needs to be taken into consideration that the reliable weighing of bananas at this stage was especially difficult due to the previously explained issues with tray weights. A possible reason for the drying characteristics of chilies over night could be that hot air from daytime experiments was stored inside the chili's hollow core or inside the vegetable itself. This might have led to drying processes happening from inside of the chilies. The highest amount of weight was lost when storing the chilies in sealed black plastic bags outside the dryer, possibly because they were better insulated from cold ambient air.

5.2 Solar Dryer Components

Comparative experiments revealed that the new dryer's performance has significantly increased compared to the previous design and open-air drying. Hence, improvements achieved through the improved design were confirmed.

Material acquisition to build the solar dryer's components was rather easy in this case due to the possibility of going to India. In more remote locations, this is likely more difficult and time-consuming. Hence, the best solution would be to set up one fixed manufacturing place and transport the completed solar dryers to the respective farms. If that is not possible, it might be necessary to customize the material selection depending on availabilities. The same applies to sourcing of spare parts.

Heat Exchanger and Absorber

Average heat exchanger efficiency laid around 36 % taking both cold and hot side into consideration. Leakage values were estimated at around 31 % which is considerably low taking into account that the dryer was built out of simple materials and no advanced sealing techniques were applied.

The absorber increased the airflow's temperature right at the beginning of the experiments by at least 5 °C. Short after, the efficiency drops as the dryer's components need to warm up before reaching operating temperatures. Until midday, when solar irradiance reaches its peak the temperature difference between absorber in- and outlet increases and declines after. The absorber's efficiency is strongly linked to irradiance which is what makes this external parameter very crucial.

Drying Chamber and Fan Setups

Plotting the average and maximum temperatures in different drying chambers under various fan setups revealed several interesting outcomes. Without active circulation (no internal fan), chambers 1 and 8, located closest to the absorber, recorded the highest temperatures, while chambers 4 and 6, positioned further away, had the lowest. Refer to Figure 3-7 for chamber numbering. When using the big fan (Setup No. 2 and No. 3 - refer to Table 3-3 for overview of fan setups), the air mixed more evenly, resulting in the lowest temperature range among setups. In the backward spinning setup, chamber 8 recorded the highest temperatures, aligning with the anticipated airflow as illustrated in Figure 3-8. Here, hot air from the absorber is directed towards chambers 8 and 6, with the remaining flow heating chambers 1 and 4.

For the reversible fans (Setup No. 4 and No. 5), a distinct trend emerged: with only one reversible fan and hence lower forced circulation, chamber 1 had the highest and chamber 6 had the lowest temperatures, while chambers 8 and 4 achieved similar values. Adding a second reversible fan increased internal flow, leading to similar temperatures in chambers 1 and 8, while chambers 4 and 6 remained cooler. The limited spinning duration of one minute for reversible fans might explain the temperature differences. Extending this duration could potentially result in more uniform air mixing, similar to the big fan setup, but at higher temperature levels, thus enhancing the uniformity of the drying process.

Heat Storage

Experiments on heat storage performance did not yield promising results. While it was confirmed that sufficient thermal energy was stored in the water bottles to exceed the temperature of the air leaving the absorber after nine hours, the heat storage could not maintain a high enough temperature inside the dryer to sustain the drying process. Table 4-1 illustrates that chili weight reduced more when stored in plastic bags outside the dryer, compared to when the dryer operated with installed heat storage.

Another potential benefit of the heat storage was the reduction of peak temperatures to prevent overheating. However, the highest recorded temperatures inside the drying chamber did not exceed the recommended drying range of 50 °C – 60 °C (see Figure 4-22).

There is potential for improvement by modifying the heat storage setup. However, for these experiments, no enhancement was observed by installing the heat storage. This might also change when drying different types of food.

5.3   Drying Characteristics and Uniform Drying

When comparing different drying configurations, one significant tradeoff became apparent. The drying process was either fast, encompassing a high drying rate or uniform with a considerably lower drying rate. In order to choose the best-suited setup, individual requirements need to be assessed.

The experiments revealed potential for using reversible fans. In addition to fan type, the position inside the dryer also needs to be taken into account. The highest impact was recorded for the uppermost trays. Having additional fans in the lower sections might increase uniformity.

Nevertheless, increased cost, energy consumption and availability have to be considered when evaluating such options. Since it was not possible to reliably measure the airflow inside the solar dryer, false assumptions regarding flow patterns are possible.

It turned out that the produce's characteristics had a big impact as well, and different dryer settings are more beneficial for different fruit or vegetable.

In general, it was often difficult to identify causes for certain outcomes as there were many different factors influencing the results. Not only external parameters such as weather but also ripeness and condition of the produce varied in each experiment. The increased shading caused by the house's roof throughout the course of experiments (see Figure 4-4) is also a good example of unforeseen circumstances that had an impact on the results. Even though all experiments were conducted within two months, the shift in the earth's position relative to the sun resulted in increased sun altitudes and therefore extended the shading period in the morning.

Assessing humidity measurements at the dryer revealed that optimal levels for drying banana and chili can be achieved. Suggested RH values lie between 30 % and 40 % and the measure values ranged between 33 % and 35 %. Ideal drying temperatures range between 50 °C and 60 °C. These conditions could only be reached during peak times.

6   Conclusion and Outlook

6.1   Conclusion

The experiments conducted for this thesis aimed to improve solar drying techniques to enhance the preservation of agricultural produce in Bhutan. The goal was to further develop an indirect solar dryer with a focus on achieving uniform drying. Despite some unforeseen challenges, the study revealed promising outcomes and identified areas needing further improvement.

Various internal fan configurations were tested to compare their impact on airflow patterns and drying rates. The findings indicate that while reversible fans show promise in enhancing airflow and drying efficiency, further investigation is needed to fully understand their potential. Experiments with different fan setups revealed a tradeoff between fast and uniform drying.

A comparative analysis of drying bananas and chilies revealed that each comestible has different drying requirements and characteristics. Bananas, with their higher moisture content, dried faster but required careful monitoring, while chilies, which dried slower, needed extended drying times to achieve the desired preservation. Optimal drying conditions could be achieved, but only temporarily. These differences underscore the importance of customizing drying parameters based on the type of produce.

Furthermore, findings suggest that external conditions, such as solar irradiance, significantly impact drying efficiency. Higher irradiance correlates with better drying performance, emphasizing the need to consider weather conditions in the design and operation of solar dryers.

Additionally, the study highlighted the need for reliable methods to measure airflow inside the dryer and control drying conditions to ensure consistent product quality.

In summary, the results demonstrated that it is possible to build a well-performing solar dryer using locally available materials. Optimizing fan setups and understanding the impact of external conditions are key to improving solar drying efficiency. These findings provide valuable insights for designing more effective and reliable solar dryers, contributing to better preservation of agricultural produce.

6.2   Further Research and Development

To build on the findings of this research, several areas for future improvement and investigation were identified:

Laboratory Testing, Field Testing and Real-World Application

- Conduct experiments in controllable laboratory environment first
    - to determine dryer's performance under ideal conditions to identify if drying of certain produce is feasible (Can ideal drying temperature and RH be reached? How long is drying time until produce is safe to store? etc.).
    - to detect possible challenges before conducting field tests.
- During field tests in Dewathang, Bhutan: Move dryer to different (unshaded) position.
- Gather feedback from local farmers to understand practical challenges and adapt the design accordingly.

Airflow and Ventilation

- Find a way to measure and/or simulate airflow inside dryer.
- Conduct further experiments to optimize the placement and operatiotwos to achieve more uniform airflow.

Component Efficiency

- Further improve efficiency by exploring different design adjustments (bigger absorber, more trays inside the dryer, surface treatments, etc.).
- Refine the design and materials used for the heat storage to enhance thermal retention and release.
- Investigate alternative materials and configurations that could improve the efficiency of the heat storage.
- Consider supplying fans with solar power to eliminate the need for external electricity entirely.

Material and Financial Considerations

- Further investigate locally available materials that could reduce costs while maintaining or improving the dryer's performance.
- Evaluate the long-term durability and maintenance requirements of different components to ensure sustainability.

Expand Research Scope

- Extend experiments to include a broader range of fruits and vegetables to validate the dryer's versatility.
- Conduct market analysis to assess the economic viability and potential impact of the improved solar dryer on local farmers and communities.

III   References

Atkins, P.W., Paula, J.D., Keeler, J., 2018. Atkins' Physical Chemistry. Oxford University Press.

Çengel, Y.A., Ghajar, A.J., 2020. Heat and mass transfer: fundamentals & applications, Sixth edition in SI Units. ed. McGraw Hill, New York.

Chhogyel, N., Kumar, L., 2018. Climate change and potential impacts on agriculture in Bhutan: a discussion of pertinent issues. Agriculture & Food Security 7, 79. https://doi.org/10.1186/s40066-018-0229-6

Dandamrongrak, R., Mason, R., Young, G., 2003. The effect of pretreatments on the drying rate and quality of dried bananas. International Journal of Food Science & Technology 38, 877–882. https://doi.org/10.1046/j.0950-5423.2003.00753.x

Davidsson, H., Olsson, J., Phinney, R., Bernardo, L.R., Otte, P., Tivana, L., 2017. Towards a Homogenous Drying Rate Using a Solar Fruit Dryer. pp. 1–7. https://doi.org/10.18086/swc.2017.24.01

Ekechukwu, O.V., Norton, B., 1999. Review of solar-energy drying systems I: an overview of drying principles and theory - ScienceDirect. Energy Conversion and Management 40, 615–655. https://doi.org/. https://doi.org/10.1016/S0196-8904(98)00092-2

Getahun, E., Delele, M.A., Gabbiye, N., Fanta, S.W., Vanierschot, M., 2021. Studying the drying characteristics and quality attributes of chili pepper at different maturity stages: Experimental and mechanistic model. Case Studies in Thermal Engineering 26, 101052. https://doi.org/10.1016/j.csite.2021.101052

Inyang, U., Oboh, I., Etuk, B., 2017. International Journal of Food Nutrition and Safety, 2017, 8(1): 45-72 International Journal of Food Nutrition and Safety Drying and the Different Techniques 8, 45–72.

Jamtsho, T., Om, D., 2023. Design, Analysis and Performance Evaluation of Indirect Solar Dryer. (2023).

JNEC, 2020. About The College. Jigme Namgyel Engineering College. URL https://www.jnec.edu.bt/en/our-college/ (accessed 3.21.24).

Joardder, M.U.H., Hasan Masud, M., 2019. Food Preservation in Developing Countries: Challenges and Solutions. Springer International Publishing, Cham. https://doi.org/10.1007/978-3-030-11530-2

Johansson, P., Svensson, A., 1999. Metoder för mätning av Luftflöden i ventilationsinstallationer. Byggforskningsrådet, Lund.

Kuepper, F., 2024. CAD model of dryer's improved design in Bhutan.

Kumar, M., Sansaniwal, S.K., Khatak, P., 2016. Progress in solar dryers for drying various commodities. Renewable and Sustainable Energy Reviews 55, 346–360. https://doi.org/10.1016/j.rser.2015.10.158

Kumar, P., Singh, D., 2020. Advanced technologies and performance investigations of solar dryers: A review. Renewable Energy Focus 35, 148–158. https://doi.org/10.1016/j.ref.2020.10.003

Mahmoodi, H., 2023. The Development and Testing of Low-Cost Heat Transfer Enhancements for Solar Dryers. (2023).

Mat Desa, W.N., Mohammad, M., Fudholi, A., 2019. Review of drying technology of fig. Trends in Food Science & Technology 88, 93–103. https://doi.org/10.1016/j.tifs.2019.03.018

Ministry of Agriculture, 1992. Review of the Bhutan National Research System: The Renewable Natural Resource Sector. Ministry of Agriculture, Thimphu.

Ministry of Health Bhutan, 2021. NATIONAL NUTRITION STRATEGY AND ACTION PLAN (2021-2025). Department of Public Health, Bhutan.

National Statistics Bureau, 2022. 2022 Labour Force Survey Report Bhutan (Survery Report). National Statistics Bureau.

National Statistics Bureau, 2021. 2021 Agriculture Survey Report. National Statistics Bureau.

Probert, A., 2022. Development and testing of a novel solar dryer design with an incorporated heat exchanger - For use in the Himalayan regions. (2022).

Rissler, C., 2023. Mitigating Post-Harvest Losses in Bhutan through Solar Food Drying: Optimization and Analysis.

Robin, 2023. Traditional vs Modern Techniques of Food Preservation: Understanding the Pros and Cons - FoodieScapes. URL https://foodiescapes.com/preserving-food/techniques-of-food-preservation/ (accessed 6.1.24).

Srikiatden, J., Roberts, J., 2007. Moisture Transfer in Solid Food Materials: A Review of Mechanisms, Models, and Measurements. International Journal of Food Properties 10. https://doi.org/10.1080/10942910601161672

Wagner, W., Pruss, A., 1993. International Equations for the Saturation Properties of Ordinary Water Substance. Revised According to the International Temperature Scale of 1990. Addendum to J. Phys. Chem. Ref. Data **16** , 893 (1987). Journal of Physical and Chemical Reference Data 22, 783–787. https://doi.org/10.1063/1.555926

WorldAtlas, 2024. The World's 10 Most Mountainous Countries [WWW Document]. URL https://www.worldatlas.com/geography/the-world-s-10-most-mountainous-countries.html (accessed 4.10.24).